NASA TECHNICAL TRANSLATION NASA TT F-15,168

NON-STEADY-STATE SHOCK WAVE FRONTS AND THEIR INTERACTION

Sebastian von Hoerner

Translation of "Instationare Stossfronten und Ihre Wechselwirkung," Fortschritte der Physik, Vol. 6, No. 7-8, 1958, pp. 375-425.

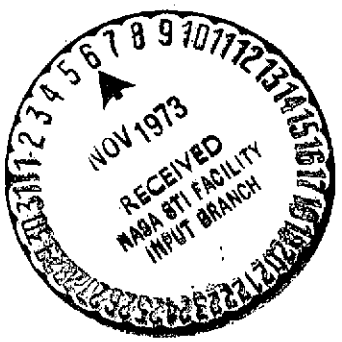

NATIONAL AERONAUTICS AND SPACE ADMINISTRATION
WASHINGTON, D.C. 20546 NOVEMBER 1973

STANDARD TITLE PAGE

1. Report No.	2. Government Accession No.	3. Recipient's Catalog No.
NASA TT F-15,168		

4. Title and Subtitle	5. Report Date
NON-STEADY-STATE SHOCK WAVE FRONTS AND THEIR INTERACTION	November 1973
	6. Performing Organization Code

7. Author(s)	8. Performing Organization Report No.
Sebastian von Hoerner Astronomisches Rechen-Institut, Heidelberg	10. Work Unit No.

9. Performing Organization Name and Address	11. Contract or Grant No.
Leo Kanner Associates, P.O. Box 5187 Redwood City, California 94063	NASw-2481
	13. Type of Report and Period Covered
	Translation
12. Sponsoring Agency Name and Address	14. Sponsoring Agency Code
National Aeronautics and Space Administration, Washington, D.C. 20546	

15. Supplementary Notes

Translation of "Instationare Stossfronten und Ihre Wechselwirkung," Fortschritte der Physik, Vol. 6, No. 7-8, 1958, pp. 375-425

16. Abstract The results of a team effort, led by von Weizsäcker, on shock waves and their interactions are reported. If a single planar strong shock wave is propagated in a gas of uniform density and velocity and no large supply of momentum is applied from behind, all initial distributions of density, velocity and temperature behind the front approach the same distribution, called the standard solution, asymptotically after a short period. It is identified with a homology solution with critical value k_o of the homology parameter; values other than k_o lead to singularities in density or temperature at finite distances. Approximately linear velocity distributions are obtained. Radiation loss is calculated and applied to astronomical data. The limiting case of very strong radiation yields the nonsteady "isothermal shock wave." A study of shock waves in magnetic fields indicates the existence of three different kinds of waves. Sample calculations are made for the interaction of two nonsteady, parallel, strong shock waves. The treatment of a field of interacting shock waves with Monte Carlo methods is outlines.

17. Key Words (Selected by Author(s))	18. Distribution Statement
	Unclassified - Unlimited

19. Security Classif. (of this report)	20. Security Classif. (of this page)	21. No. of Pages	22. Price
Unclassified	Unclassified	79	

NON-STEADY-STATE SHOCK WAVE FRONTS AND THEIR INTERACTION

Sebastian von Hoerner
Astronomisches Rechen-Institut, Heidelberg

Introduction

/376*

A study group was formed at the Max-Planck-Institut für Physik, Göttingen, in 1953 under the direction of C.F. v. Weizsäcker, consisting of about 8 members working closely on the problem of strong shock wave fronts. Impetus for this was provided by the necessity of searching for a sort of "theory of turbulence with supersonic velocities" applicable to many problems in astrophysics. Due to a variety of considerations, this was not attempted with the otherwise conventional, direct approach of correlation statistics, but began with the details; and what amount to the (rather fictive) turbulence elements in the case of subsonic velocity would correspond, in the case of supersonic velocity, to (phenomenologically better-defined) shock wave fronts.

An additional impetus for concern with shock wave fronts is provided directly by observation. The photographs of several emission nebulae exhibit a large number of filamentous structures, and it is quite possible that some of these filaments could be interpreted as laterally projected shock wave fronts or as lines of intersection between two obliquely intersecting fronts.

Since then, ten articles from this study group have been published. Additional existent material includes three unpublished dissertations, two more articles, and a series of other discussions and results. This study group has now been disbanded again. A certain preliminary stopping point

*Numbers in the margin indicate pagination in the foreign text.

has been reached within our working program. Further pursuit would only be feasible with renewed "large-scale implementation," and we hope that this idea will be taken up again in some other study group and continued.

Thus the goal of this article is to summarize everything to date and to unify it so that it can serve as a basis for renewed study. An additional reason for such a summary is that, aside from the pursuit of our direct program, we have attacked and worked on a large number of individual questions in hydrodynamics which could also be useful for completely different problems.

I. Problem and Program

1. Purpose

For many problems in astrophysics, a need has existed for several years for a theory of turbulence at supersonic velocities. As an example, we would like to briefly outline the conditions of motion of interstellar matter. The interstellar matter which is highly concentrated in the plane of the Milky Way consists primarily of atomic hydrogen; its density averages about 10^{-24} to 10^{-23} g/cm^3. We distinguish between the unionized HI regions, with temperatures of 50-100° absolute, and the ionized HII regions, at about 10,000°. The associated sonic velocities are thus about 1 km/sec (for HI) and 10 km/sec (for HII). We must compare these with the flow velocities. The interstellar matter participates in the general rotation about the center of the Milky Way, which amounts to about 250 km/sec in the vicinity of the Sun. On this rotation is superimposed a disordered motion (individual regions or clouds) on the order of 5 km/sec; however, individual fast clouds can have velocities up to 100 km/sec. We can find even higher velocities in expanding shells following supernovae, e.g. 1000 km/sec in the Crab nebula.

We can see from this comparison that the Mach numbers M (flow velocity / sonic velocity) characterizing the state of motion are generally scattered over the wide range between 1 and 100. On the other hand, theoretical works to date on turbulent motion processes include an assumption of incompressibility ($M \ll 1$), so their results can only be applied in special cases, if at all.

A purpose is thus clearly provided for seeking a theory of turbulence at high Mach numbers; and the question now is by what path to best approach this theory. We could first

consider proceeding much as in the incompressible case, for example, by conducting a Fourier analysis in accordance with Heisenberg [1], by considering a hierarchy of elements within one another in accordance with v. Weizsäcker [2], or by introducing correlation tensors in accordance with Chandrasekhar [3, 4]. The compressibility now to be included would have to be accounted for with suitable additional terms.

It is highly questionable, however, whether a formulation of this nature can produce success. As soon as three-dimensional velocity differences become greater than sonic velocity, shock wave fronts must necessarily be generated which represent something essentially new relative to the incompressible case, and we can quite generally suppose that for this reason alone, statements concerning the one case cannot be applied to the other. We shall cover this point in greater detail below, however.

2. Energy Dissipation

In derivations of the theory of incompressible turbulence, it has generally been necessary to introduce a similarity postulate, such as in the following form: "If L is the diameter of the largest and l_0 is that of the smallest turbulence elements, then within the orders of magnitude characterized by $l_0 << l << L$, the magnitude of energy which is dissipated (per g and per sec) from elements on the order of l, e.g. to elements on the order of $l/2$, should not be a function of l." We offer the two articles by Chandrasekhar cited above [3, 4] as an example: while the hope is expressed in the former article that such a similarity statement would not have to be postulated in the future, but could be derived, it still had to be expressly postulated in the second article. /378

For clarification of this point, let us consider the derivations of formulae in [3, 4]. Use has been made of the principles of continuity and the conservation of momentum, but not that of the conservation of energy. And it appears evident that we cannot obtain an unequivocal description of reality from just the former two principles. Thus the principle of the conservation of energy must also be employed in some form. Its use in direct form would probably mean studying the processes of energy dissipation in detail and building up the entire field of turbulence stepwise, starting with the smallest elements. And this rather tedious approach could only be avoided if the introduction of similarity postulates proved to be adequate and successful.

Whereas the introduction of a similarity postulate possessed some quite plausible features, this is no longer the case for high Mach numbers. Due to the occurrence of shock wave fronts of all orders of magnitude, a portion of the energy is converted directly into heat from each order of magnitude, not just via the smaller and smallest elements, as before. It might be possible to take these circumstances into consideration with a modified form of the postulate, but we also wish to point out another objection (and one which appears more serious to us).

Let us consider the magnitude and the whereabouts of the dissipated energy. If turbulence elements of diameter l have velocity w relative to their surroundings, then almost their entire energy is dissipated during time l/w, i.e. about $(1/2)w^2$ (erg/g). Except for factors on the order of 1, dissipation S (erg/g·sec) amounts to

$$S = w^3/l$$

(Since, in the case of incompressibility, S also may not be dependent upon l, according to the similarity postulate, we obtain the Kolmogoroff spectrum of turbulence from this: $w \sim l^{1/3}$.) After passage through smaller and smaller elements, this energy is finally converted into heat. A corresponding input of energy to the largest elements is then necessary to maintain a steady state.

In the incompressible case, M << 1 also implies: turbulence energy << thermal energy. This means, however, that the increase in thermal energy caused by dissipation is relatively small, and the resultant timewise increase in temperature can be neglected.

This is no longer the case for M > 1. Turbulence energy is now greater than thermal energy, and the increase in thermal energy during time l/w is greater than its original magnitude. Expressed in clearer terms: if I stir the gas in a vessel around at supersonic velocity, the temperature will have risen in just two or three rotations, due to dissipation, to such an extent that the sonic velocity has now become higher than the velocity of stirring (M < 1). Thus a steady state with M > 1 can only be maintained if provisions are made for extremely rapid removal of the thermal energy generated. /379

In practice, this removal of energy takes place via radiation from within the shock waves. And since the shock wave fronts of all orders of magnitude will radiate energy, it appears reasonable that a statistical analysis of the state of motion could only be possible if express consideration were given to the presence and the effect of shock wave fronts.

In order to illustrate this statement, we finally point out that for M > 1, the spectrum of turbulence (or a law corresponding to it) must be a function of the ratio between the energies which are radiated by shock wave fronts of different extent. And this necessarily leads to a detailed consideration of processes within the shock wave fronts.

Let us insert an additional remark here. The rapidity of energy removal through radiation which is required for a steady state with M > 1 should only be possible with complete ionization, i.e. at front temperatures of T_F > 10,000°K. For M >> 1 and atomic hydrogen, T_F is related to front velocity V in the case of no radiation, according to formulae (2) and (3), by

$$T_F = 22{,}5\, V^2 \quad \left| \begin{array}{l} T_F \text{ in } ^\circ\mathrm{K} \\ V \text{ in km/sec.} \end{array} \right.$$

It follows from this that a steady state with M > 1 should only be possible for velocities above 20 km/sec.

3. Working Program

The following program was worked out for v. Weizsäcker's study group on the basis of considerations such as the above:

a) First, treatment of the problem of the strong, non-steady, planar shock wave front which (as the simplest case) moves in a quiescent region ahead of it of constant density.

b) Study of the radiation of energy from within the shock wave, as well as its reverse effect on the distribution of density and temperature behind the front.

c) Concerning additional complications, primary consideration of the effect of magnetic fields.

d) The next problem concerns the various types of interaction between two shock wave fronts, first of type a), as well as with the radiation of energy and perhaps also with magnetic fields.

e) After clarification of all of these individual problems, an attempt to find a steady state whose characteristics can be described completely and statistically for a field of shock wave fronts passing through one another in unordered fashion in all directions, at all velocities and of all sizes (with a suitable input of energy). /380

If it had proved possible to succeed all the way through item e), we would thus have obtained a theory of turbulence at high Mach numbers. It can easily be seen, however, that this is a long and quite complex path to the goal being sought.

What has so far been achieved with this approach will be briefly summarized here: Item a) can be considered to have been completed. From almost any initial distributions, a "standard front" develops after a brief period; this could also be treated analytically as a homology solution of a certain type. The class of homology solutions and the associated problem of transformation groups was studied in detail, as well as the problem of the stability of the homology solutions.

Regarding item b), an article on stationary shock wave fronts with energy radiation has been completed but not yet published, and the same is true of an article on the isothermal limiting case for nonsteady fronts.

Regarding item c), the effect of magnetic fields of arbitrary strength and direction upon stationary fronts of arbitrary strength has been completely covered.

Regarding item d), the interactions of two strong, non-steady, parallel standard fronts have been calculated.

Along the lines of item e), a highly simplified model has been treated by Monte Carlo methods in order to achieve a first overview of the manner in which steady states can eventually be established.

We shall report on the work outlined here in the following sections.

II. The Nonsteady, Strong, Planar Front

The motion of a nonsteady shock wave front and the distribution of velocity u, density ρ and pressure p behind the front are described by a system of three partial differential equations of the hyperbolic type, along with the boundary conditions which apply at the front. Let t be time, x be position (in the direction of the front's propagation), and a subscript indicate the corresponding partial derivative. Then, in Eulerian notation, neglecting viscosity and thermal conductivity, our basic equations read

$$\left.\begin{array}{ll} \text{Conservation of mass} & \varrho_t + u\varrho_x + \varrho u_x = 0 \\ \text{Conservation of momentum} & u_t + uu_x + \dfrac{p_x}{\varrho} = 0 \\ \text{Conservation of energy} & p_t + up_x + \varkappa p u_x = 0 \end{array}\right\} \tag{1}$$

and, at the front, we have the following boundary conditions /381 for a strong shock (M >> 1) (e.g. see [5]):

$$\left.\begin{array}{l} \varrho = \dfrac{\varkappa+1}{\varkappa-1}\varrho = 4\varrho_0 \\ p = \dfrac{\varkappa-1}{2}\varrho u^2 = \dfrac{1}{3}\varrho u^2. \end{array}\right\} \tag{2}$$

The number of boundary conditions is 1 less than the number of basic equations because the front is reached by exactly one characteristic of the region behind it, and thus only two degrees of freedom remain. The position of the front in each case must be calculated by the integration of an additional equation

$$V = \frac{\varkappa+1}{2}u = \frac{4}{3}u \tag{3}$$

where ρ_0 is density ahead of the front, V is the velocity of the front itself, and κ is the ratio of specific heats. With

a view toward our astrophysical application, we have used the value for a monatomic gas, $\kappa = 5/3$. We collect Eqs. (2) and (3) under the heading "front conditions."

The problems associated with the above equations are, first of all, of a technical mathematical nature: the equations are not linear, and the position of the boundary depends upon the solution itself. Secondly, no specific solution has yet been indicated by the equations used so far; we still require initial distributions of u, ρ and p, or general conditions which restrict the type of solution. Thirdly, we are not interested in some special solution, but would like to obtain as general information as possible in accordance with our working program.

The intent of this section is to study the extent to which the description of shock wave fronts can be simplified mathematically in a physically reasonable manner in order to ultimately formulate general statements. One such possibility is the elimination of certain types of solutions by reducing the system of partial differential equations (1) to a system of ordinary differential equations by means of a separation theorem (compatible with the front conditions). This approach yields so-called homology solutions. For them to be physically meaningful, the values of u, ρ and p must remain finite for all finite x; and if it is to be of interest to us in terms of our problem, a solution must be stable (neighboring solutions must osculate with increasing time). If both requirements are satisfied, then it can be hoped that this type of solution is approached asymptotically from various initial conditions and thus represents a useful description of shock wave fronts occurring in nature.

A second possibility consists of the direct numerical treatment of partial system (1) by allowing the widest variety of initial distributions to follow their course and observing whether they become more similar to one another with time and approach a common form of solution. Both possibilities were tried at Göttingen, and their joint result was given the name "standard solution." /382

To avoid having to again interrupt the presentation of the homology solutions, we wish to begin with a description of the second possibility.

A. System of Partial Differential Equations with Initial Conditions

1. Computation Method

The development of various initial distributions with time was studied in an article by Hain and v. Hoerner [6]. It was first necessary to determine here whether to use Eulerian or Lagrangian coordinates for this purpose. For adiabatic gas motion without external forces, a Lagrangian representation would actually be the more natural and more appropriate mode of description, since entropy then remains constant in the time direction, and since direct use is made here of the concept of particle trajectories and the fact that they cannot overlap. It was found, however, that the formulation of boundary conditions then becomes more complex and that their numerical treatment requires involved and time-consuming operations. This is because the Lagrangian coordinates are totally unsuitable for describing a front through which matter passes (in a quantity determined only by the solution itself). Thus after several attempts, we gave preference to the Eulerian representation.

The next question is whether to calculate with a uniform time interval, or along characteristics. Since we also need the positions of the characteristics in the former case, for the stability of calculations, and since the only computer available at that time, G 1, is better exploited with the characteristics method, the latter was given preference. The distributions of u, ρ, and p sought at fixed times were then obtained by linear interpolation within the network of characteristics.

It was more convenient for computation here to replace the dependent variables ρ and p with the variables a and s (sonic velocity and normalized entropy),

$$a^2 = \varkappa \frac{p}{\varrho}, \quad s = \ln\left(\frac{p}{\varrho^{\varkappa}}\right);$$

System (1) then reads

$$\left.\begin{aligned} &u_t + uu_x + \gamma_0 \cdot aa_x + \gamma_1 \cdot a^2 s_x = 0 \\ &a_t + ua_x + \frac{1}{\gamma_0} \cdot au_x = 0 \\ &s_t + us_x = 0 \end{aligned}\right\} \tag{4}$$

where

$$\gamma_0 = \frac{2}{\varkappa - 1} = 3 \quad \text{and} \quad \gamma_1 = -\frac{1}{\varkappa(\varkappa - 1)} = -\frac{9}{10}. \tag{5}$$

The two boundary conditions now read /383

$$a = \gamma_2 \cdot u \quad \text{and} \quad s = \gamma_3 + 2\ln u \tag{6}$$

where

$$\gamma_2 = \sqrt{\frac{\varkappa(\varkappa - 1)}{2}} = \frac{\sqrt{5}}{3} \quad \text{and} \quad \gamma_3 = \ln\left[\frac{\varkappa + 1}{2\varrho_0^{\varkappa - 1}}\left(\frac{\varkappa + 1}{\varkappa + 1}\right)^{\varkappa}\right], \tag{7}$$

while the third front condition (3) remains unchanged.

System (4) has three real characteristics, whose directions are found to be

$$C^+ = u + a, \quad C^- = u - a, \quad C^0 = u \qquad (8)$$

The remainder of the approach can only be outlined briefly here. The hodograph equations were used in differential form along the characteristics; each C^+ characteristic was calculated all the way from the initial distribution to the front. Then the next starting point on the initial distribution in each case was selected in such a manner that the changes in the front values did not exceed a maximum quantity. Second-order calculations were made; the method is described in detail in [6].

2. Testing for Homology

We investigated whether, with increasing time, the solutions so calculated approach an approximately constant form. As we shall show in Section B2, this amounts to the question of whether the solutions approach one of von Weizsäcker's homology solutions [5]. Making use of von Weizsäcker's homolgy theorem, we can also formally assign a value k of the homology parameter to every point (x,t) in any arbitrary (non-homologous) solution, and the existence of homology is indicated by k(x,t) = const. The system of equations for those quantities from which k(x,t) is calculated is overdetermined here; with an adjustment we then obtain both k(x,t) and a measure of error σ(x,t). For homology we must require not only k(x,t) = const but also σ(x,t) = 0.

3. Results

The first question is, for what type of initial distribution can we expect a development of constant conditions, since almost any arbitrary timewise front behavior can ultimately

be produced by a suitably selected initial distribution. Although it cannot be stated precisely in mathematical terms, it appears evident that constant conditions can only develop from arbitrary initial conditions (if at all) if the region to the rear is also largely determined by the front, alone. Thus no appreciable resupply of momentum may occur from the rear. For this reason, all examples calculated were selected in such a manner that the resupply of momentum to the rear is somehow limited, e.g. by a steep dropoff in velocity, density or temperature. Within this one condition, however, the examples have been selected with the greatest possible variety. /384 In practice, this means that we allow a single fast cloud of finite extension to the rear, behind which no other cloud is following, to enter a quiescent gas of constant density.

Overall, nine examples were calculated, three of which are shown in Fig. 1. In all nine cases, the timewise behavior of k along the front, k(X), initially exhibits pronounced fluctuations but, after a relatively short time, gradually assumes a constant value, which was found to be the same for all examples and averaged $k = 0.39 \pm 0.01$. The next test was to also calculate k(x,t) for the region behind the front. The result was the same: after initially pronounced fluctuations, the constant (in terms of space and time) average value of

$$k = 0.390 \pm 0.006 \qquad (9)$$

was eventually assumed.

For the third test, Fig. 2 shows the curves of $\sigma(x,t)$ averaged over all calculated examples, indicating deviation from homology. The times used here were determined from the front behavior of k (right side of Fig. 1) as follows:

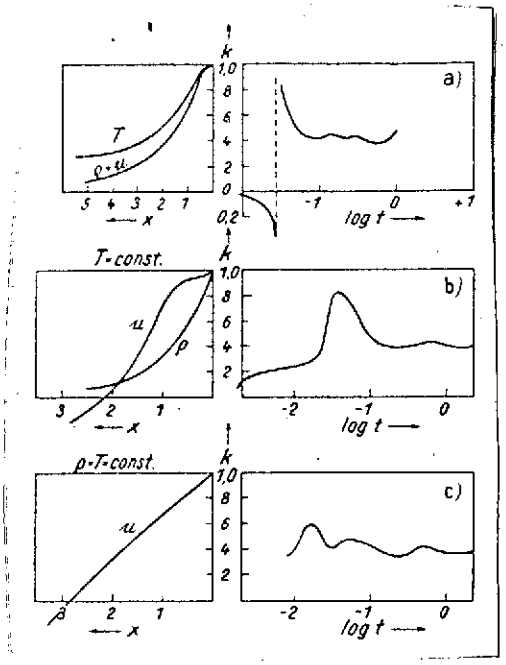

Fig. 1. Left: three arbitrarily selected initial distributions of density, velocity and temperature behind the front. Right: the resultant time curves of the (formally defined) homology parameter k along the front. From [6].

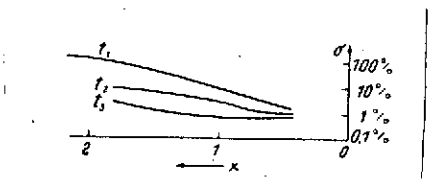

Fig. 2. Deviation σ(x,t) from homology, averaged over all nine calculated examples, at the time points defined by (10). The x-scale is always normalized so that u_x/u assumes the same value at the front. From [6].

t_1 = time of greatest deflection of k(X)

t_2 = time at which k(X) = 0.39 reached (10)

t_3 = latest possible point in time, $\sim 5t_2$.

We see from Fig. 2 that the feasibility of representation by means of a homology solution decreases with increasing distance from the front for each fixed point in time and increases with increasing time for each fixed front distance. /385 The homology solution which is approached is thus gradually assumed with time from the direction of the front. (The residual value σ = 1% corresponds to computational precision).

In addition, the osculation of the region behind it to the approached homology solution was followed graphically for all examples. E.g., Fig. 3 shows temperature curves at various times for the first of the distributions in Fig. 1. We see how the homology solution develops from the direction of the front.

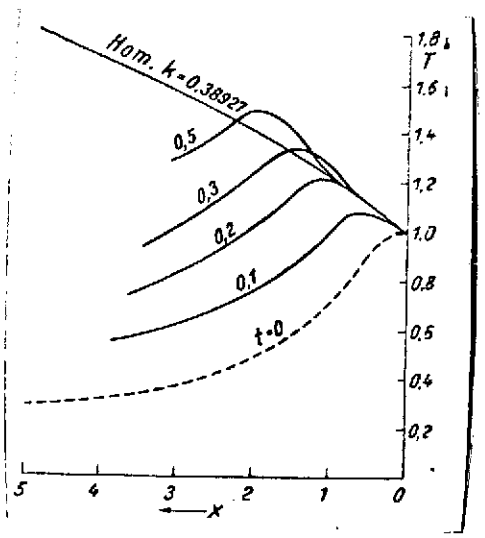

Fig. 3. Temperature of the region behind front ((initial distribution in Fig. 1a) approaches the standard solution with increasing time. Front temperature is always normalized to 1; x-scale as in Fig. 2. From [6].

4. The Standard Solution

Our results are thus as follows: The same homologous solution ($k \sim 0.39$) is always approached in all nine cases calculated. This solution, which was always approached in the absence of a resupply of momentum, was given the name "standard solution." While it had previously been assumed that all plane homology solutions had singularities for finite x, the standard solution exhibited a completely regular, smooth shape even very far to the rear. Inspired by this, Häfele [13] found the singular solution to the homolgy equations described in the next section, which remains regular as the one homology solution for all finite x.

One of the examples calculated was followed to long times, /386 in large time intervals (computational outlay increases with the square of time!), and was then compared with Häfele's solution. Figure 4 shows the results: within its computational precision, the distribution which is assumed is identical with Häfele's solution.

In explanation of Figs. 3 and 4, it should also be mentioned that all quantities have been normalized in terms of their front values. The x-scale has been normalized in such a manner that the derivative of normalized velocity with

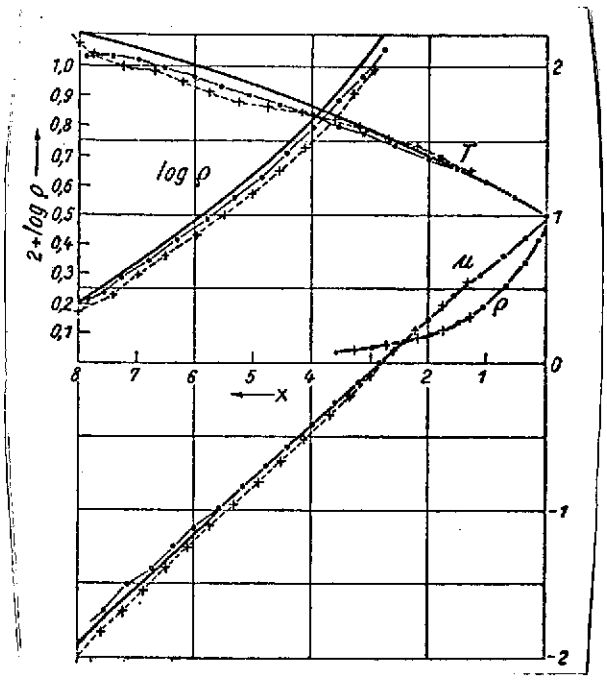

Fig. 4. The distribution assumed (from an arbitrary starting distribution) at two time intervals: +++++ t = 8.9; ..... t = 16.8. Standard solution according to Häfele plotted as heavy curve for comparison. From [6].

respect to position is always given the same value at the front. This normalization was introduced so that various distributions could be checked for similarity.

In the search for as simple a mathematical description of the standard solution as possible, we were initially struck by the almost linear curve of velocity. Moreover, the following are good approximations for the normalized (as described above) quantities:

$$\varrho = \left(1 + \frac{x}{3}\right)^{-3} \tag{11}$$

and

$$p = \varrho^{0.821}. \tag{12}$$

The question of the "linear solutions" raised here will be treated separately in Section C.

B. The Homology Solutions

1. The "Block Wave"

In order to achieve a first, rough overview of the manner in which the velocity of a strong shock wave front left to itself decays, von Weizsäcker [5] represented the front and the region behind it schematically with a "block" of spatially

constant density ρ and gas velocity u, assumed to be of finite thickness d perpendicular to the front. The region ahead of it is assumed to be quiescent and of constant density. Due to front conditions (2) and (3), ρ = const and V/u = const while, due to the accumulation of matter (of the region ahead), u and V decrease with time and d increases.

For the accumulation of matter, $\dot{m} = \rho(V - u) = \text{const} \cdot u$, where m is the mass of the block per cm^2 front area, and the correspondingly defined momentum of the block is J = mu. The requirement of the conservation of momentum is thus

$$\left.\begin{aligned} \dot{J} = \dot{m}u + m\dot{u} = \text{const} \cdot u^2 + \dot{u}J/u = 0 \\ \dot{u} = -\text{const} \cdot u^3 \end{aligned}\right| \qquad (13)$$

or

and, integrated, with V - const·u,

$$V(t) = \frac{\text{const}}{(t - t_0)^{1/2}}. \qquad (14)$$

If we impose the requirement of conservation of energy, /387 mu^2 = const, however, then instead of the above, we obtain

$$V(t) = \frac{\text{const}}{(t - t_0)^{1/3}}. \qquad (15)$$

The difference in the two exponents shows the shortcomings of this model; the form of dependence upon time, which is common to both results, suggests, however, that an expression of the type

$$V(t) = \frac{\text{const}}{(t - t_0)^k} \qquad (16)$$

could also be successful for an exact treatment of the problem. We will see below that this supposition proves correct (with

k = 0.389) and was thus able to indicate the proper approach even for this rough model.

2. General Derivation of the Homology Theorem

Von Weizsäcker proceeds directly from the statement suggested by [16], which he extended in a corresponding manner to the region behind the front, making use of the spherically symmetrical homology theorems of Taylor [7] and Guderley [8, 9]. We wish to present a derivation of the homology theorem here, however, which starts only with a very widely applicable physical requirement and which is kept as general as possible, so that its result can no longer appear in any manner to be an arbitrary mathematical statement.

We are actually interested in the question of whether a type of solution exists which, starting from various initial distributions, is always (or under certain conditions) approached asymptotically with time. If this is the case, then the solution should remain similar to itself from there on. Let this be our physical requirement, and the next question is how we are to formulate this similarity requirement mathematically. We wish to keep the theorem just as general as possible, and we believe the least that we must require of a solution which "remains similar to itself" to be the following:

> The functional relationship between the quantities u, ρ and p, normalized with their front values, shall be the same at all times. (17)

If we call X the time-dependent position of the front, then this means

$$\frac{u(x,t)}{U} = f\left\{\frac{\varrho(x,t)}{R}\right\} = g\left\{\frac{p(x,t)}{P}\right\} \quad (18)$$

where

$$U = u(X), \quad R = \varrho(X), \quad P = p(X).$$

(If not otherwise expressly noted, we wish to adopt the convention that large letters shall always be functions of time only.) This requirement is identical with the following formulation:

The values of u, ρ and p at one time should result from /388
the values at another time via an arbitrary (not necessarily linear!) time-dependent scale transformation of u, ρ, p and x.

Or, in formulae,

$$\left.\begin{aligned} \varrho(x,t) &= R(t)\cdot r(\xi) \\ u(x,t) &= U(t)\cdot \varphi(\xi) \\ p(x,t) &= P(t)\cdot \psi(\xi) \\ \xi &= \xi(x,t) \\ \xi(X) &= \text{const} = c, \end{aligned}\right| \qquad (19)$$

with

where ξ is an arbitrary function of position and time which always assumes the same value c at the front.

If we now also take the three front conditions (2) and (3) into consideration, our homology requirement finally reads

$$\left.\begin{aligned} \varrho(x,t) &= r(\xi) \\ u(x,t) &= U\cdot \varphi(\xi) \\ p(x,t) &= \frac{1}{3}\,U^2\cdot \psi(\xi). \end{aligned}\right| \qquad (20)$$

If we agree to assume density $\rho_0 = 1/4$ ahead of the front, then

$$r(c) = \phi(c) = \psi(c) = 1 \qquad (21)$$

We now apply our statement (20) to differential equation (1) and obtain the following (the prime symbol indicates derivation with respect to ξ):

$$\left.\begin{aligned} &\frac{\xi_t}{U\xi_x}\cdot r' + r\varphi' + \varphi r' = 0 \\ &\frac{\xi_t}{U\xi_x}\varphi' + \frac{\dot{U}}{U^2\xi_x}\varphi + \frac{1}{3}\frac{\psi'}{r} + \varphi\varphi' = 0 \\ &\frac{\xi_t}{U\xi_x}\psi' + \frac{\dot{U}}{U^2\xi_x}2\psi + \frac{5}{3}\psi\varphi' + \varphi\psi' = 0. \end{aligned}\right| \qquad (22)$$

Since r, ψ and ϕ are supposed to be functions of ξ only, the requirement of separability means that

$$-\frac{\dot{U}}{U^2\xi_x} = g'(\xi) \text{ and } \frac{\xi_t}{U\xi_x} = h(\xi) \qquad (23)$$

are also functions of ξ only, which we label g' and h. If, for the purpose of abbreviation, we define

$$W = 1/U,$$

the first requirement yields

$$\dot{W} = g'(\xi)\cdot\xi_x.$$

Integrating over x, with B as an arbitrary time function, we obtain /389

$$\dot{W}x + B = g(\xi),$$

and if we call γ the inverse function of g, then

$$\xi = \gamma(\dot{W}x + B).$$

Since ξ only occurs as the argument of arbitrary functions, however, it is no limitation on generality to state the following identity for the arbitrary function γ:

$$\xi = \dot{W}x + B. \qquad (24)$$

Without our having required it at the start, we thus find that the scale transformation must be linear in x.

When (24) is used, the second separability requirement reads

$$\frac{W(\ddot{W}x+\dot{B})}{\dot{W}} = h(\xi) = h(\dot{W}x+B),$$

and since the left side is linear in x, the right side must likewise be:

$$h(\dot{W}x+B) = a\dot{W}x + aB + b; \quad a, b = \text{const.}$$

By a comparison of coefficients with the left side, after double integration over t ($0 \neq a \neq 1$), we obtain

$$W = \text{const}\cdot(t-t_0)^{1/(1-a)}, \quad \dot{W} = \text{const}\cdot W^a, \quad B = \text{const}\cdot W^a + \text{const.}$$

Our result thus finally assumes the form

$$\xi = \frac{x-x_0}{(t-t_0)^{1-k}} \text{ and } U = \frac{U_0}{(t-t_0)^k}; \quad 1 \neq k \neq \infty, \tag{25}$$

where we have set $k = 1/(1-a)$; x_0, t_0, U_0 and k are constants.

We note that k is the only important constant here (= homology parameter); for the excluded values of k, we also add the solutions which result instead of it and obtain

Type	$U(t)$	$\xi(x,t)$
a. General	t^{-k}	$x\cdot t^{-a-b}$
b. $(k=1)$	t^{-1}	$x \pm \ln t$
c. $(k=\infty)$	$e^{\pm t}$	$xe^{\pm t}$.

(26)

Formula (25) is precisely von Weizsäcker's homology theorem, which we have derived here from physical requirement (17), kept quite general.

It is interesting that we can obtain the same result from a completely different and purely mathematical starting point. Thus von Hagenow [10], proceeding from Lie's theory [11] and an article by Lax [12], studied the invariance of the basic equations (1) relative to infinitesimal transformations of /390 the dependent and independent variables. Through the relationship between invariance properties and separability, von Hagenow obtains the totality of all separation theorems which follow from the invariance properties of (1). If we pick out only those theorems which are compatible with front conditions (2) and (3), we get precisely our three forms (26), while the remaining five cannot be employed to represent shock wave fronts with a constant region ahead. Thus for all five of the remaining theorems, for example, temperature is a pure function of ξ and would therefore be constant with time at the front.

An additional result of von Hagenow's work is the following general statement: A separation theorem is always compatible with the front conditions if the region behind and the region ahead of the front can be separated on the basis of the same theorem. It should also be noted that we obtain homology solutions only in the limiting case of the strong front; at least, derivations and theorems have not so far been possible for the case of general front strength.

3. The Homology Equations

The reduction of system (1) of partial differential equations to a system of ordinary differential equations is accomplished by also substituting (26a) into (22), as von Weizsäcker does [5]. Overall, we have thus substituted statement (20) and the resultant special form (26a) into basic equations (1). We obtain the system

$$\left.\begin{aligned}
[\varphi-(1-k)\xi]\cdot r'+r\varphi'&=0\\
[\varphi-(1-k)\xi]\cdot\varphi'+\frac{1}{3}\frac{\psi'}{r}-k\varphi&=0\\
[\varphi-(1-k)\xi]\cdot\psi'+\frac{5}{3}\psi\varphi'-2k\psi&=0.
\end{aligned}\right| \qquad (27)$$

This notation differs formally from that in [5] somewhat, but is identical to it. Comparison with the similar formulations by Guderley [9] and by Courant-Friedrichs [14] is carried out in [5]. System (27) was integrated numerically for various k by von Weizsäcker, three different types of solution being obtained.

Häfele continues the analytical treatment of (27) in [13], starting with a method developed by Guderley and applied there to the spherically symmetrical case [8]. The decisive aspect of this method is the reduction of system (27) to one first-order differential equation and two subsequent quadratures.

We introduce the new dependent variables[1] (n = 1 - k)

$$\nu(\xi)=\frac{\varphi(\xi)}{n\cdot\xi}\ \text{and}\ \ \mu(\xi)=\left(\frac{\varkappa}{n^2\xi^2}\cdot\frac{\psi(\xi)}{r(\xi)}\right)^{1/4}, \qquad (28)$$

while only $\ln r$ is used in place of the third dependent variable. We replace the derivatives with respect to ξ with those with respect to $\ln\xi$. If we substitute this into (27), a system of equations for the functions ν, μ and $\ln r$ results in which the coefficients of the derivatives are functions of ν and μ, only, not of r and ξ. The first of equations (27), for example, becomes

/391

[1] Here, μ is related to sonic velocity a by

$$(\nu - 1)\frac{d\ln r}{d\ln \xi} + \frac{d\nu}{d\ln \xi} + \nu = 0, \tag{29}$$

while the two other equations assume similar forms, but become so complex that we do not wish to present them here. This property of the system, that its coefficients are functions of μ and ν only, has the consequence that a differential equation in μ and ν can be obtained. It is given in Häfele such that spherically symmetrical and cylindrically symmetrical cases can also be covered; we merely wish to formulate it here for the planar case in which we are interested,

$$\frac{d\mu}{d\nu} = \frac{\mu}{\nu - 1} \cdot \frac{\mu^2\{\varkappa(\nu-1)+n'\} + \varkappa(\nu-1)\left\{\nu\left(\frac{3-\varkappa}{2n}+\frac{1+\varkappa}{2}\right) - \nu^2 - \frac{1}{n}\right\}}{\mu^2(\varkappa\nu + 2n') - \varkappa\nu(\nu-1)\left(\nu - \frac{1}{n}\right)} \tag{30}$$

where $n = 1 - k$ and $n' = 1 - \frac{1}{n}$.

With a suitable choice of density in the region ahead of the front, front conditions now take the form

$$\nu = 2/(\varkappa + 1) = {}^3/_4 \tag{31a}$$

$$\mu = \sqrt{2\varkappa(\varkappa - 1)}\,/(\varkappa + 1) = \sqrt{5}/4 \tag{31b}$$

$$\ln r = 0.$$

This means that all solutions which represent the region behind a strong front pass through a fixed point A in the μ,ν diagram whose coordinates are a function only of the ratio of specific heats κ.

The variables μ and ν introduced in (28) are indeed suitable for a certain region behind the front, but not in the vicinity of ξ = 0. For this reason projective coordinates

are introduced, as in Guderley, with

$$\mu = x_1/x_3, \quad \nu = x_2/x_3, \quad x_3 = \text{const} - x_1/3 + x_2/3, \tag{32}$$

from which a quite complex differential equation of the form

$$dx_2/dx_1 = g(x_1, x_2, x_3) \tag{33}$$

is obtained, which can be referred to in [13]. The variables x_1, x_2 are in turn undefined within a certain region lying very far behind the front, however, so we must again use variables μ, ν here.

Thus either system (27) or the alternate use (depending upon region) of Eqs. (30) and (33) can be selected for integration. If we only wish the solution for certain values of κ and k, then the integration of (27) is to be preferred. On the other hand, representation on the basis of (30) and (33) is particularly suitable not only for obtaining an overview of the totality of possible solutions but also for ascertaining whether a physically regular solution is available. /393

4. Types of Solution

a) Front Behavior. In order to provide ourselves with a qualitative overview of the various types of solutions, we first consider the behavior of the front itself. According to expressions (20) and front condition (3), front velocity V(t) has the same form as U(t) in (25). We immediately see from (25) that the front is accelerated for $k < 0$, moves at constant velocity for $k = 0$, and is decelerated for $k > 0$. We thereby obtain the first line of our overview in Table 1, which has been compiled from [5, 13, 17].

TABLE 1. THE VARIOUS TYPES OF HOMOLOGY SOLUTIONS. /392

Parameter Value		$k<0$	$k=0$	$0<k<1/3$	$k=1/3$	$1/3<k<k_0$	$k=k_0$	$k_0<k<1$	$k=1$	$k>1$
The front is		accelerated	steady	decelerated						
Front moves	from	x_0	$-\infty$	x_0					$-\infty$	$-\infty$
	to	$+\infty$	$+\infty$	$+\infty$					$+\infty$	x_0
Region behind front on separatrix ...			./.	./.	III	./.	II	./.		
Rear boundary	Convergence via		./.	./.			$P_{2,3}$	Reversal line		
	toward			P_6			P_8	P_4		
	Rear boundary		./.	Impenetrable wall			Vacuum	Reversal line		
	Velocity		>0	>0	$=0$	<0	$-\infty$	<0	$=0$	>0
	Function values		ϱ, p, T = const	$\varrho=0$, $p=$ const, $T=\infty$			$\varrho=0$ $p=0$ $T=\infty$	ϱ, p, T finite, but $\varrho_x, p_x, T_x=\infty$		

[Note: ./. = not applicable.]

The second line gives us the path covered by the front; we obtain it simply by solution of (25). Since we are interested only in decaying fronts, further discussion will be restricted to $k > 0$.

b) The Directional Field of Equation (30). Further differentiation among various types is only possible if we consider the region behind the front, particularly its rear end and the singularities which occur there. For this purpose Häfele [13] gives the directional field of differential equation (30), both in the μ,ν coordinates and in projective coordinates (32). The reader is referred to the extensive study by Häfele regarding all details. We have taken our /394
Fig. 5 from the article [13] to provide a rough overview.

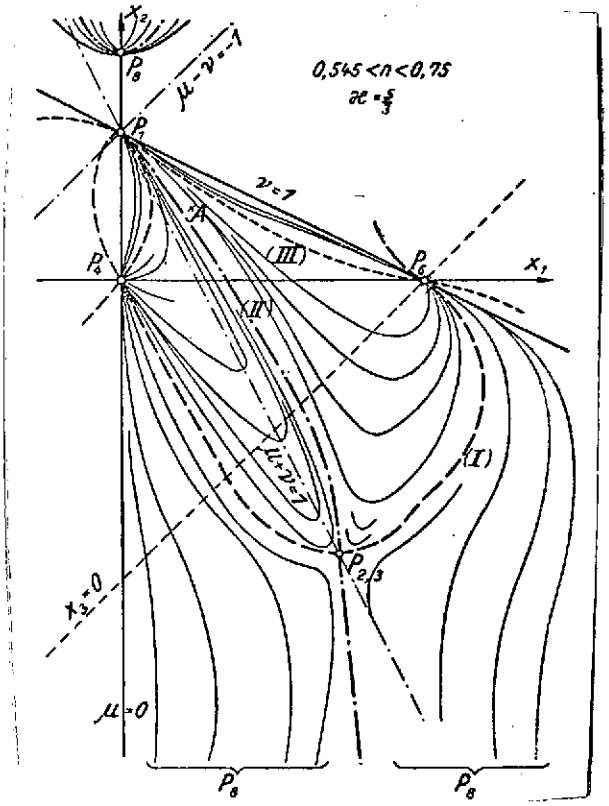

Fig. 5. Directional field of differential equation (30) in projective coordinates, from (33). For k = 1 - n = 0.38927, front point A lies on separatrix II. The standard solution begins at A and follows separatrix II through $P_{2,3}$ to P_8. From [13].

We see five singularities in Fig. 5. In general, both the positions and the character of the singularities vary with κ and k, so quite different types of directional fields apply, for example, to various domains of k. In his (unpublished) dissertation, however, Häfele made a precise survey of all possibilities and found that a physically regular solution which is of special interest to us can in any case only exist in the directional field associated with the region

$$\frac{\varkappa-1}{\varkappa+1} < k < \frac{\varkappa}{\varkappa+2}, \quad \text{i.e. } 0{,}25 < k < 0{,}454 \text{ for } \varkappa = \frac{5}{3}. \tag{34}$$

Figure 5 applies to this region. The front itself is represented by point A. Since the coordinates of point A are a function of κ, and the behavior of the solutions is a function of κ and k, the following different possibilities exist for the position of A in the field of solutions, depending upon the choice of the two parameters:

A lies:

1. to the right of separatrix III
2. on separatrix III
3. between III and II
4. on separatrix II
5. to the left of II.

The solution which passes through A here proceeds toward P_6 in the first three cases, via $P_{2,3}$ toward P_8 in the fourth case, and toward P_4 in the last case. The path toward P_4 leads over the line $\mu + \nu = 1$, however, which represents a reversal line.

c) The Nature of the Singularities. The problem of the reversal lines is treated extensively by Tollmien [15, 16] and Guderley [9] and is summarized by Häfele in [17]. The type with which we are dealing is merely designated "reversal line with expansion"; it cannot be realized physically with any initial and boundary conditions. In mathematical terms, it is characterized by the fact that, for constant t, the solution cannot exceed a certain $\bar{x}_c$ and becomes a closed curve, i.e. becomes two-valued. A clear, but inexact, representation would be that in which matter is sucked up from the rear at x_c. To be exact, however, this would have to occur at supersonic velocity, but this is physically impossible. Thus case 5 must be ruled out for our program.

On the other hand, let us consider the convergence of solutions toward P_6. According to Häfele, this point is located at ξ = const, i.e. at finite x. At it, $\rho = 0$, $p =$ = const and $T = \infty$. From the fact that temperature becomes infinite[2], Häfele calls P_6 an "energy resupply." We do not

[2] In [20], Häfele presents a solution which approaches P_6 with finite temperature. It does not satisfy the front conditions, however.

consider this to be totally correct. Since pressure equalization has already occurred (p = const) and since thermal conductivity is neglected in all cases, no thermal energy is likewise introduced at P_6. We would rather derive another interpretation of P_6. To this end we study the question as to whether matter passes through P_6 or not. We designate gas velocity at P_6 as U_6 and the velocity of point P_6 itself as V_6. /395

1. Convergence toward separatrix III. Since $x_2 = 0$, then, with (32), $\nu = 0$. With (28) and (20), we then also have $U_6 = 0$. According to Häfele [13], $\xi = 0$; i.e., from (25), $x_6 = \text{const} = 0$ and thus $V_6 = 0$. We thus obtain $U_6 = V_6$; no matter passes through P_6.

2. Convergence with $\nu = 1$ (Fig. 5). According to Häfele, $\xi = \text{const}\ (=\xi_6)$ here; by differentiating (25) we obtain

$$V_6 = (1 - k) \cdot \xi_6 / t^k.$$

On the other hand, $\nu = 1$ and $\xi = \text{const}$ yield, in accordance with (28) and (20),

$$U_6 = U_0 (1 - k) \cdot \xi_6 / t^k.$$

By substituting (28), (25) and (20) into front condition (3) -- and by comparing the result with (31a) -- we can see that ν is normalized in Häfele's article in just such a manner that it presumes the normalization of $U_0 = 1$. Thus here again, and thus in all cases,

$$U_6 = V_6 \tag{35}$$

We can therefore interpret P_6 as a rear boundary consisting of an impenetrable wall. Since this wall is motionless at $k = 1/3$ (since $\nu = 0$), this case is suitable for describing shock waves produced by planar explosion at a fixed wall. (The corresponding case of a spherical explosion has

been solved analytically by Taylor [18]. In [19], Culler and Fried point out the possibility of approximating conditions in a shock tube with this solution, k = 1/3.

We must rule out convergence toward P_6 for the problem associated with our program, however, since no fixed walls exist in the cosmos. We must look for a solution which represents free flowoff to the rear. The only solution with this property is, according to Häfele, separatrix II, which we will cover in the next section.

5. The Standard Solution

If we wish to avoid convergence toward P_6, we see from Fig. 5 that the solution must cross the line $\mu + \nu = 1$. This is only possible in a physically regular manner, however, at singularity $P_{2,3}$, i.e. only on separatrix II. The numerical solutions (for various κ) obtained by Häfele go past $P_{2,3}$ quite smoothly for ρ, p, T and u, and further convergence toward P_8 can be interpreted as free flowoff into vacuum.

Häfele was even able to give the analytical solution for the special value $\kappa = 7/5$ (close to the value applicable to air), which we wish to show here in abbreviated form for fixed time only (α = const): /396

$$\left.\begin{aligned} u &\sim 1 + \frac{5\alpha}{2}\xi \\ T &\sim 1 + \alpha\xi \\ p &\sim (1+\alpha\xi)^{-5/2} \\ \varrho &\sim (1+\alpha\xi)^{-3/2}. \end{aligned}\right| \qquad (36)$$

The value of k associated with separatrix II will be called k_o below. For $\kappa = 7/5$ we obtained $k_o = 2/5 = 0.4$.

Quite extensive computations were necessary for other values of κ: With various values selected for k, integration was carried out from A until the solution turned to the right or left in front of $P_{2,3}$; we were thereby able to gradually approach k_o. Table 2 shows the results.

TABLE 2. HOMOLOGY PARAMETER k_o FOR THE STANDARD SOLUTION WITH VARIOUS SPECIFIC HEAT RATIOS κ.

κ	k_0
1,1	0,43112 $\pm$ 0,00001
1,4	0,4
5/3	0,38927 $\pm$ 0,000005
2,8	0,373296 $\pm$ 0,000005

We have already shown the distribution of u, ρ and p in the standard solution in Fig. 4 for $\kappa = 5/3$. It is tabulated in Häfele [13], and the distributions are also shown there in the form of figures for other values of κ. Behind the front, u, ρ and p always decrease monotonically, while temperature increases sharply for small values of κ, only gently for $\kappa = 5/3$, and decreases monotonically for $\kappa = 2.8$. A striking feature is the curve of velocity u, which in all cases is almost (for $\kappa = 7/5$, exactly) linear and whose slope is also only very slightly dependent upon κ. We shall return to this in Section C.

Singularity $P_{2,3}$ is not distinguished by anything in the distribution of u, ρ and p,[3] but is in the pattern of characteristics. All C^+ characteristics passing through the front and $P_{2,3}$ reach the front after finite time, whereas no characteristic from the region behind $P_{2,3}$ reaches the front. This means, however, that the front is no longer in any way affected by the region behind $P_{2,3}$; thus the behavior of the front is not

[3] In Fig. 4, $P_{2,3}$ is at x = 6.4.

affected by how the solution is continued behind $P_{2,3}$. And since $P_{2,3}$ itself moves along a C^+ characteristic, the entire region lying between $P_{2,3}$ and the front is unaffected by the region behind $P_{2,3}$. (Provided only that, say, additional shock wave fronts are not generated behind $P_{2,3}$.) We have thus come closer to the question posed in Section II,A,3: "From what initial distributions can a standard solution eventually be assumed?" The answer is: "When a C^+ characteristic which only reaches the front at $t = \infty$ begins within the initial distribution selected." We cannot immediately see whether this is the case or not from the initial distribution, and we must thus be satisfied with the qualitative condition of no resupply. /397

C. Linear Solutions

1. Starting Point

We pointed out in the preceding section that the standard solution which is eventually assumed exhibits a velocity curve which is approximately linear in x for all values of κ for which calculations were made. The curve is in fact exactly linear at $\kappa = 7/5$. Thus the question arises as to whether, first of all, basic hydrodynamic equations (1) can be solved generally with the additional requirement

$$u(x,t) = Ax + B \tag{37}$$

(upper-case letters = functions of time only) and, secondly, whether the "linear solutions" so obtained are suitable for the approximate description of shock wave fronts. This has been studied by the author in [21].

2. Results

It was found that we can give the general solution to (1) under requirement (37). We wish merely to present the results here; they have the form:

$$\left.\begin{aligned} u(x,t) &= u_0 + \dot{S}\cdot y \\ \varrho(x,t) &= S^{-1}\cdot\Phi(y) \\ p(x,t) &= S^{-\gamma}\cdot\Psi(y) \\ y(x,t) &= \{x - u_0(t-t_0)\}/S. \end{aligned}\right| \qquad (38)$$

where

Here, u_o and t_o are constants, and time function S is given by

$$\ddot{S}S^{5/3} = \alpha = \text{const} \qquad (39)$$

Φ and Ψ are functions of y; one of these is arbitrary; the other is given by the relation

$$\Psi'/\Phi = -\alpha y \qquad (40)$$

It was also found that entropy is a pure function of y, and this means that the lines y = const are "life lines" (particle trajectories). We could thus also conceive of (38) as a special separation theorem in Lagrangian coordinates.

Expression (39) is easily integrated. Depending upon the choice of α and an additional integration constant β, we obtain the three general solution types 1, 4, 6 in Fig. 6, while dashed /398 lines 2, 3, 5 represent limiting cases. (Thus in the case of solution 5, for example, u = 0 for t = ∞.)

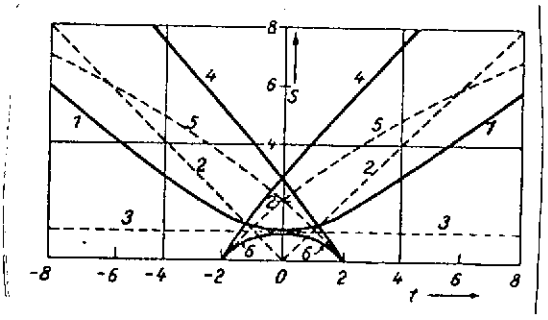

Fig. 6. Solutions to the Eulerian equations with a linear velocity curve. The distance S between neighboring "life lines" is plotted over time t. From [21].

The second striking characteristic of the standard solution is that, as a good approximation, pressure is proportional to a power of density for a very broad region behind the front:

$$p(x,t) = P(t)\cdot\rho^{\gamma}, \text{ where} \qquad (41)$$

γ = const;

we obtained $\gamma \sim 0.8$. For

this reason, a similar approach was used in [21] to study whether the general solution to (1) could be given if requirement (41) were applied instead of supplementary requirement (37). It was found here that (37) follows from (41) and (1). This means, however, that the solutions singled out by (41) are a subgroup of linear solutions. Thus (38) and (39) again apply, except that now no function of y is arbitrary any more: density is a power, determined by γ, of an expression which is quadratic in x.

3. Application

It was possible to show that the front conditions are not compatible with requirement (37) except at $\kappa = 7/5$; see (36). The linear solutions are quite suitable, however, for an approximate representation of the rearward region of the standard solution, especially its subgroup (41), which again holds exactly at $\kappa = 7/5$. For a linear solution, u_x must be a constant and, due to (40), $(p_x/\rho)_x$ = const likewise, while subgroup (41) also requires that γ = const. We ask how much these quantities deviate from constancy in the case of the standard solution, and give the magnitude of deviation in percent, relative to the value applicable at the front, in Table 3. Velocity u has been used as a comprehensible scale; it is normalized to 1 at the front, drops off to the rear and becomes negative. The region which is of interest for application probably lies within the interval $+1 > u > -1$, in which density falls off by as much as a factor of 30. Table 3 shows that within this region, all requirements are still satisfied relatively well. An additional example of a linear solution is isentropic flowoff into vacuum as treated by Burgers [22] and Pack [23]. If we consider a quiescent gas of constant density and entropy in the half-plane $x > 0$ and vacuum in $x < 0$ at $t = 0$, then a widening transition zone propagates on both sides of $x = 0$ for $t > 0$, in which velocity is a linear function of position.

TABLE 3. DEVIATIONS IN THE STANDARD FRONT AT $\kappa = 5/3$ RELATIVE TO THE LINEAR SOLUTIONS. /399

n	u_x	$(p_x/\varrho)_x$	γ
0	+ 2%	− 6%	+ 1,3%
− 1	+ 4%	− 24%	+ 2,3%
− 3	+ 7%	− 47%	+ 4,0%
− 10	+ 11%	− 83%	+ 6,2%

In summary, it appears as if flowoff processes into the vacuum exhibited the general tendency toward linear flowoff, slighly perturbed under some circumstances by boundary conditions not compatible with it.

D. The Stability of the Standard Solution

A solution will be considered stable if neighboring solutions approach this solution asymptotically with increasing time. It was found in Section II,A,3 that all nine quite varied initial distributions actually do approach the standard solution asymptotically; this can be taken as a strong argument in favor of its stability. On the other hand, this type of "experimental mathematics" is of course not capable of providing real evidence of stability. The purpose of this section is thus to seek analytical evidence of stability. Since this question cannot yet be considered satisfactorily answered, we shall cover it only briefly.

1. F. Meyer's Treatment [24]

For the purpose of analyzing the timewise development of any solutions, F. Meyer introduces the derivatives with respect to position, made dimensionless, at the particular front position:

$$\left.\begin{aligned} \alpha &= (u_{xx}\, u/u_x^2)_{\text{Front}} \\ \beta &= (u_{xxx}\, u^2/u_x^3)_{\text{Front}} \\ \gamma &= (u_{4x}\, u^3/u_x^4)_{\text{Front}} \end{aligned}\right| \qquad (42)$$

as well as the derivative, made dimensionless, in the direction of the front curve,

$$\frac{d}{d\eta} = \frac{1}{u_x} \cdot \left(V \frac{\partial}{\partial x} + \frac{\partial}{\partial t} \right).$$

The system of ordinary differential equations can then be derived (for $\kappa = 5/3$) from basic equations (1) and front conditions (2) and (3):

$$\left.\begin{aligned} \frac{d\alpha}{d\eta} &= -0{,}416\beta + 0{,}8\alpha^2 - 1{,}35\alpha - 0{,}0519 \\ \frac{d\beta}{d\eta} &= -0{,}41\gamma + (1{,}2\alpha - 1{,}31)\beta - 5{,}21\,\alpha^2 - 0{,}355\alpha - 0{,}0205. \end{aligned}\right| \qquad (43)$$

Both (42) and (43) could be taken to derivatives of any order. However, the equation for the n^{th} derivative always includes the $(n+1)^{th}$ derivative, so the variation in the highest derivative can never be calculated. A number of studies by Meyer have shown, however, that the higher derivatives have only a very slight effect on the low-order derivatives, so, for estimating conditions, it appeared reasonable to break off series (42) at γ, and to consider γ constant in (43). /400

We can now formally assign a homology solution to any solution by requiring agreement at the position of the front for all first and second derivatives (precisely all free parameters of the homology solution are then used up). Homology parameter k is determined by

$$1/k = 13/5 + (9/10)\alpha \qquad (44)$$

If the solution to be studied is a homology solution, then

$$\alpha = \text{const and } \beta = \text{const}$$

must hold.

We show the directional field for system (43) in Fig. 7. The heavy lines are separatrices; the perimeter is infinite distance on the α,β-plane. Let us consider singularity P_1. It is characterized by the fact that $d\alpha/d\eta = 0$ and $d\beta/d\eta = 0$ at it. Thus, due to the constancy of α and β, it represents a homology solution. In addition, only solutions entering it exist, none which leave it. This means, however, that all neighboring solutions approach the solution represented by P_1 with time. P_1 thus represents one (and indeed the only) stable solution. In actuality, γ will of course vary with time, in a manner which is not determined by the method applied. But even if we consider γ to be constant, the position of point P_1 still depends upon the choice of γ, and the same then also applies, with (44), to the resultant k. Since the relationship $k(\gamma)$ is only a very weak one, however, the uncertainty of k is likewise only slight. If only relatively small values of γ are considered, Meyer ultimately finds that

$$k = 0.39 \pm 6\% \text{ for } -1 < \gamma < +1. \qquad (45)$$

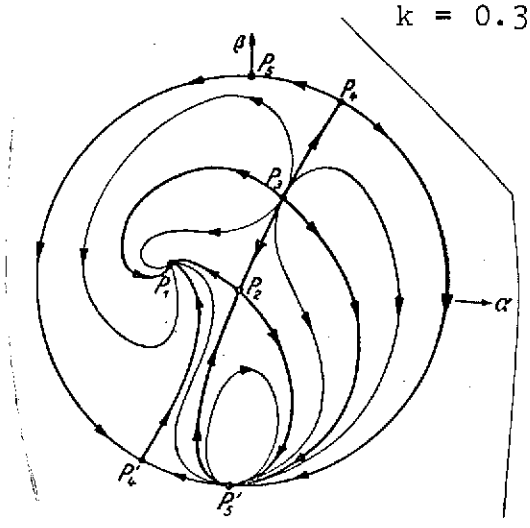

Fig. 7. Directional field for system (43). The stable solution is represented by singularity P_1. From [24].

In spite of its shortcoming (constancy of γ), this method is thus capable, first of all, of providing a good approximation for k_o ($k_o = 0.38927 \pm 0.001\%$, from Table 2) and, secondly, of indicating the stability of this solution. This, too, is of course not a proof in the strict sense; the convergence of the method could not be demonstrated for the inclusion of higher and higher derivatives in (42). Moreover, the following is still unsatisfactory: We know

/401

from the preceding sections that one physically regular (supposedly stable) solution exists, as well as a unidimensional variety of other (possibly unstable) homology solutions. The one stable solution is included in Fig. 7 (P_1), but not the variety of other homology solutions. For each value of α (and not just at the additional singularities P_2 and P_3), there should exist a solution with the property $d\alpha/d\eta = d\beta/d\eta = 0$. The reason for this lies in the arbitrary establishment of a specific value of γ.

2. Häfele's Treatment [17]

Since we believe we can refute the validity of Häfele's results by means of a counterexample, we merely wish to outline the rather complex derivation quite briefly here; we refer the reader to the original article [17] regarding all details.

In order to be able to better follow the transition from a general solution to the homology solution being sought with regard to the equilibrium establishment process, Häfele chooses a notation similar to that of homology solutions (20) and (25) or (28). And if it is thereby to be possible to also describe general solutions, it is necessary, first of all, to set

$$n = n(t). \tag{46}$$

Secondly, Häfele replaces homology variable ξ with a quantity ϕ, which we wish to call ξ^* here, however:

$$\xi^*(x,t) = x \Big/ \int_0^t n(\tau) \cdot \tau^{n(\tau)-1}\, d\tau. \tag{47}$$

At the front, once more,

$$\xi_F^* = \text{const}. \tag{48}$$

In the case of homology, $n(t) = \text{const}$, and thus ξ^* becomes identical to ξ in formula (25). Thirdly, the functions ν and μ,

defined in a manner analogous to (48), are also explicitly dependent upon time via time function n,

$$\nu = \nu(\xi^*,n),\ \mu = \mu(\xi^*,n); \tag{49}$$

this dependence upon time vanishes again in the case of homology.

Häfele also limits consideration to general solutions which lie in the nonhomologous vicinity of standard solution $n = n_o$ and for which the following three conditions apply:

A. The solution crosses the point $\mu^2 = (\nu - 1)^2$, i.e. reaches farther to the rear than the vicinity of $P_{2,3}$.

B. No second shock wave front may be generated in the region behind the first front.

C. In the vicinity of $P_{2,3}$, $\partial\nu/\partial n$, $\partial\mu/\partial n$ and $\partial \ln \rho/\partial n$ have the same sign as in the case of homology.

Under these conditions, Häfele is then able to derive the formula /402

$$dn/dt = (n - n_o)\cdot\theta;\ \theta < 0. \tag{50}$$

It states that if all assumptions are valid, n approaches n_o; that a nonhomologous solution thus approaches the latter asymptotically from the vicinity of the standard solution.

Counterexample. For clarity, we first establish that, according to Häfele, time function n(t) is related to front velocity V(t) by

$$V = n t^{n-1}\cdot \xi_F^* = \text{const}\cdot n t^{n-1}. \tag{51}$$

Secondly, Eq. (50) states that if $n = n_o$ at some time, then $n = n_o$ is also true at every later time. Thus the value n_o can only be approached by n(t), but cannot again be left by it.

As a counterexample we select the standard solution with a small perturbation wave, moving toward the front, added in about the center between $P_{2,3}$ and the front. Thus except for the small, spatially limited disturbance, this initial distribution is identical to homology solution n_o over the entire remaining region. Conditions A and C should thus be satisfied. Moreover, the perturbation is assumed to be small and "flat" enough to also satisfy condition B. Thus (50) should apply.

We now consider the behavior of the front. During the time in which the perturbation has not yet reached the front, the behavior of the front is that associated with the standard solution. Thus during this time, $n = n_o$ according to (51). At the time at which the perturbation exerts an effect upon the front and alters its velocity, according to (51), $n \neq n_o$. This contradicts (50), however.

Discussion. We wish to present two reasons for this failure. First: it can be shown that statements (46) through (49) are still not sufficient to describe general solutions. Thus, in our example, $n = \text{const} = n_o$ until the perturbation has reached the front. During this time we also have $\xi^* = \xi$ (for all x) and, according to (49), ν and μ should then be constant along the lines $\xi = \text{const}$ of the unperturbed standard solution (likewise for all x). Once a line $\xi = \text{const}$ is reached by the perturbation, however, this statement becomes incorrect.

Secondly, what condition C actually means appears to be somewhat unclear. On the one hand, we could object that $\partial\nu/\partial n$

is a time derivative in the nonhomologous case, whereas the homology solutions are constant with time. In the nonhomologous case, on the other hand, the variation in ν in the vicinity of $P_{2,3}$ is related via the derivative $\partial\nu/\partial n$ to the variation in n at the position of the front, in accordance with (51), which does not appear to be very meaningful.

In [25], Häfele provides a proof of stability, carried out in an analogous manner, for Guderley's [8] spherically symmetrical compression shock. Here, too, it is possible to raise the same objections as those just discussed.

In summary, our critique can be formulated so as to show that in the case of Häfele's theorem, the explicit time dependence of the functions ν, μ and $\ln\rho$ degenerates not only (permissibly) in the case of homology being sought for all x, but also (impermissibly) for every bounded time interval within /403
which front velocity temporarily follows a homology solution for any rearward region. Thus the general solution cannot be described with this theorem, nor the general vicinity of the standard solution. To be sure, a special type of nonhomologous neighboring solutions may exist which is covered by the theorem. The proof of stability would be valid for this type if it proved possible to clarify condition C.

III. The Strong Front with Radiation Loss

We showed in Section I,1 that velocity u and Mach number M fall approximately within the intervals

$$5 < u < 1000 \text{ km/sec}, \quad 1 < M < 100 \tag{52}$$

for interstellar matter, and it was found in Section I,2 that a turbulence-like steady state with $M > 1$ is only possible if the heat generated by dissipation is radiated off again at a sufficient rate. Thus the purpose of this section is to study the radiation process of fast shock wave fronts in detail, as well as the effect of this radiation on the distributions of density and temperature behind the front.

Radiation processes have already been treated by Pikelner [26], but various hydrodynamic aspects were neglected. Hertweck [27] therefore undertook a new treatment of energy radiation, taking the hydrodynamic requirements into consideration; he restricted himself to the case of the steady front. His results were then to assume the role of front conditions for the nonsteady case, but this has not yet been undertaken.

Since radiation "cuts off" temperature, so to speak, von Hagenow [28] studied the isothermal nonsteady front as the limiting case of very strong radiation.

A. Hertweck's Treatment [27] of the Radiation of Energy

Hertweck treats the case of a planar, strong, steady shock wave front which enters a quiescent region ahead of it of constant density. Hertweck uses the following values for the density, temperature and degree of ionization σ of the region ahead:

$$\left.\begin{aligned} n_0 &= 1\ \text{Atom/cm}^3 \\ T_0 &= 100\ ^\circ\text{K} \\ \sigma_0 &= 0{,}01. \end{aligned}\right| \qquad (53)$$

Calculations relating to hydrodynamics and electron density are made only with pure atomic hydrogen, while helium and an admixture of heavy elements are considered with regard to radiation processes.

The individual cross sections and radiation functions were taken from the available literature and usually approximated by simple interpolation formulae. The resultant differential equations were solved numerically. Since space considerations make /404
it impossible to discuss the extensive calculations and estimates here, we merely wish to provide a rather qualitative description of Hertweck's results.

1. The Front

As before, we consider the actual shock wave front to be only the region of the thickness of several free path lengths within which the translational energy (relative to the motionless front) of the matter in the region ahead is converted into thermal energy. Since only a pure directional dispersion is involved, only a few collisions are required for this. An energy loss due to radiation or ionization can not yet occur, since the electrons (at a given velocity) have less energy, by a factor of $m_H/m_e = 1830$, than the hydrogen atoms and protons, and since the latter assume ionization cross sections on the order of 10^{-16} cm^2 only at velocities above 1000 km/sec.

We thus obtain temperatures for the atoms and ions which can be calculated from our own modified front conditions (2) and (3),

$$T_A(0) = 22.5V^2, \qquad (54)$$

where front velocity V is to be measured in km/sec and the temperature T_A of neutral hydrogen atoms and protons at the position of the front (x = 0) is measured in degrees absolute. If we replace front velocity V with Mach number $M = V/a_0$, we obtain,

$$T_A(0) = T_0 \frac{5}{16} M^2 \qquad (55)$$

where a_0 = sonic velocity ahead of the front and T_0 = temperature ahead of the front.

Density also jumps by a factor of 4 in accordance with (2) without change.

2. Establishment of Temperature Equilibrium

Only a few collisions are likewise necessary in the case of electrons for pure directional dispersion, but energy exchange proceeds slower by a factor of about m_H/m_e. The more energy the electrons receive, the sooner they also lose energy again through excitation and ionization. Thus an equilibrium temperature $T_e(x_1)$ for the electrons is established within a distance x_1 behind the front. This equilibrium-establishment process is shown in Fig. 8; the values in (53) have been used for the region ahead of the front.

An estimate indicated that for the orders of magnitude involved, it is permissible to neglect the deviations from Maxwell distributions for electrons and atoms. It is thus reasonable to apply the concept of temperature to both. Since the temperatures of neutral hydrogen and protons differ only slightly, their (weighted) mean temperature was used as T_A. T_A is still almost /405
unchanged in the first region behind the front: $T_A(x_1) \approx T_A(0)$. Fig. 9 shows temperatures T_A and $T_e(x_1)$ as functions of front

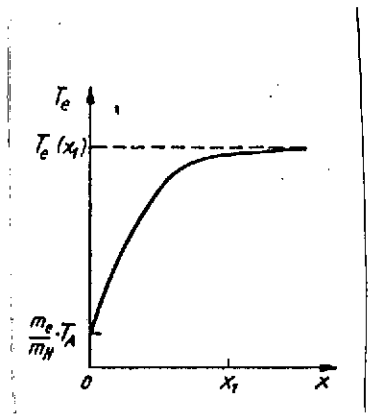

Fig. 8. Establishment of equilibrium in electron temperature T_e behind the front with the radiation of energy; $x_1 \sim 10^{16}$ cm for the values in (53). From [27].

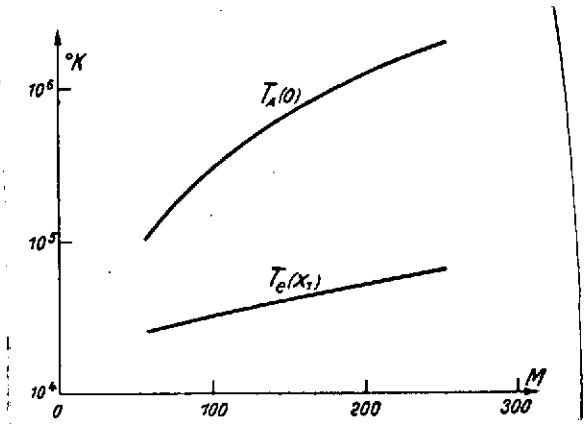

Fig. 9. Front temperature T_A of ions and H atoms, and equilibrium temperature $T_e(x_1)$ of electrons (Fig. 8), as functions of Mach number M for values in (53) for the region ahead of the front. From [27].

velocity. The relative difference between the two temperatures continually increases with increasing front velocity.

3. The Onset of Ionization

Since essentially only the electrons can "ionize," we must expect ionization to increase exponentially with time if density and temperature do not change appreciably. Since temperature /406
decreases as the result of radiation and density thus increases, the increase in ionization ultimately becomes very steep, which in turn produces a very steep dropoff in temperature and steep rise in density.

Hertweck obtains a system of three first-order differential equations for density, degree of ionization and temperature. Fig. 10 shows the results of solving numerically for the values in (53) and a front velocity of V = 100 km/sec (M = 85). The rise in electron temperature T_e up to equilibrium temperature

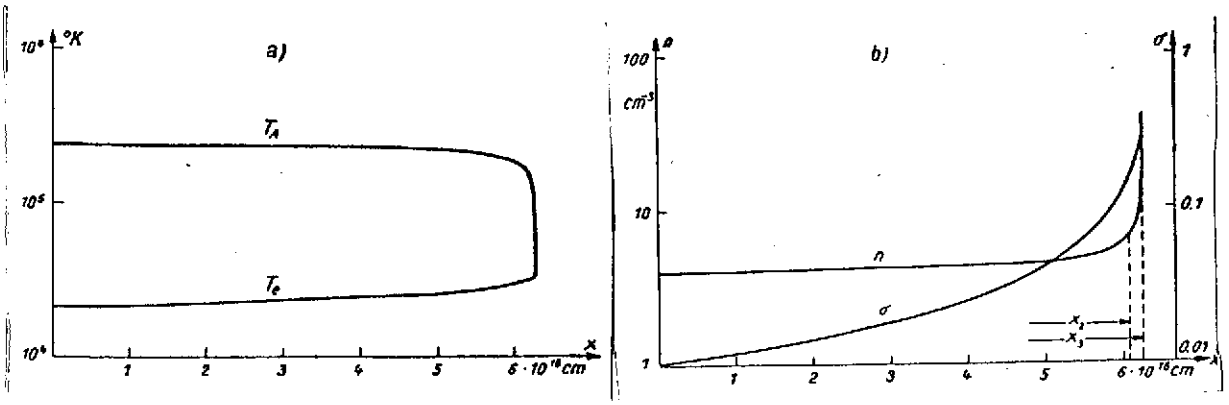

Fig. 10. a) Curves of T_A and T_e behind the front. b) The same for gas density n and degree of ionization σ.

The calculations were carried only to the point at which T_A and T_e become approximately equal. The width ($x_3 - x_2$) of the steep compression region amounts to several hundred free path lengths. From [27].

$T_e(x_1)$ has been neglected here, i.e. the calculation already starts with $T_e(x_1)$. We see the at first exponential and then steeper rise in the degree of ionization. A particularly striking feature, however, is that density remains approximately constant over almost the entire region, and increases quite steeply for the first time in a very narrow region (x_2 to x_3). The same also applies to the dropoff in temperature. The width ($x_3 - x_2$) of this compression zone is on the order of 10^{15} cm, and an estimate of the free path lengths of charged particles within this region yielded $2 \cdot 10^{12}$ cm. The compression zone is thus still several hundred free path lengths thick, and a hydrodynamic treatment of it is thus reasonable.

For $x > x_3$, temperature continues to drop off as density increases. The degree of ionization becomes approximately constant over a relatively long region, and then decreases again. Additional assumptions which concern not only outward radiation but also incoming radiation of energy are necessary for the region farther to the rear, however.

4. Comparison with Observation and Experiment

Hertweck offers the Cygnus Nebula as a possible example of strong shock wave fronts with radiation. The spectra of the nebular filaments have been studied by Chamberlain [29] and Pikelner [26]. Strong lines, compared to H_α, are found for the forbidden N II, O II and O III transitions. It has not yet proved possible to find a star in the vicinity of the nebula which is sufficiently hot for this excitation. On the other hand, the annular structures can be easily interpreted as the expanding shell of a nova explosion which took place in the past. The jacket of gases, expelled at high velocity, forms a strong shock wave front as it enters the interstellar medium; the gas in the region ahead which passes through the shock front is heated and radiates the thermal energy off again. The mass of gas moving behind the shock wave front forms the energy reservoir.

The thickness of the filaments is about $5 \cdot 10^{16}$ cm, according to [29]; even finer structures can be detected with instruments of higher resolution. Theoretically, the longitudinal scale is approximately inversely proportional to the density ahead of the front, and since this density is not known relatively accurately, it is likewise not possible to make an exact comparison with the calculated results. We can at least say, however, that reasonable orders of magnitude have been obtained.

5. Shock Tube

Kantrowitz et al. [30, 31] have generated shock waves up to Mach number M = 17 in argon; up to 40% ionization was obtained. Distances were observed between the actual front and the beginning /407 of luminescence (x_2 in Fig. 10) which fit an estimate by Hertweck well. A theoretical article by J. W. Bond has since appeared in which he treats shock wave fronts in the shock tube similarly to the manner in which Hartweck treats those in interstellar matter,

and he also obtains similar results. Additional shock wave experiments are conducted by Locte-Holtgreven et al. in Kiel [33].

B. von Hagenow's Treatment [28] of the Isothermal Nonsteady Front

Hertweck's calculation was carried out for the steady front. In order to also obtain an approximate description of the unstable case from here, we could neglect the thickness of the region lying between the front and x_3 and treat all changes in state variables as discontinuities. Thus we would again have the region ahead of the front, the front itself, and the region to the rear, with the region to the rear starting behind x_3. The applicable front conditions could be obtained from a generalization of Hertweck's results to any front conditions and any variables for the region ahead of the front, and would be functions of the chemical composition of the gas.

In the case of very strong and rapid radiation loss (and for a region ahead of the front which is already relatively hot), we can expect temperature within the newly defined front region to have decreased again to almost the temperature of the region ahead. For a sufficiently strong radiation exchange, the temperature farther behind also cannot drop below the temperature ahead of the front. It thus appears reasonable to consider the limiting case of spatially and temporally constant temperature, which yields relatively simple and understandable formulae. Von Hagenow is studying these "isothermal shock wave fronts" in a project which has not yet been completed. The work will be published in the future.

1. Basic Equations

The following are chosen for normalizing density, gas velocity and sonic velocity:

$$\left.\begin{aligned} \varrho_0 &= 1 \\ u_0 &= 0 \\ a_0 &= 1, \\ \ln \varrho &= \eta \end{aligned}\right\} \tag{56}$$

and the abbreviation

is introduced. The first two basic equations (1) then read:

$$\left.\begin{aligned} \eta_t + u\eta_x + u_x &= 0 \\ u_t + uu_x + \eta_x &= 0. \end{aligned}\right\} \tag{57}$$

In place of the third equation (1), we have substituted the constancy of temperature in the form

$$p = a_0^2 \rho = \rho. \tag{58}$$

In place of front conditions (2) and (3), applicable only to strong shocks, we now have front conditions applicable to any shock strength, /408

$$\left.\begin{aligned} \varrho &= V^2 \\ u &= V - \frac{1}{V}, \end{aligned}\right\} \tag{59}$$

where only the first equation is a boundary condition in the true sense, since here, too, the front is reached by one characteristic of the region behind. See the text regarding equation (2).

A concept of the strong front does not exist here, since the temperature of the region ahead cannot be neglected now, because T = const, in contrast to Section IIA. This is supposedly also the reason why there are no homology solutions compatible with the front conditions, as von Hagenow has shown. Consequently, there can likewise be no such simple type of "standard solution" like that in the preceding part.

2. Computational Method

A method of characteristics was selected analogous to that in Section IIA,1. The two characteristics have the directions

$$C^+ = u + 1, \quad C^- = u - 1 \quad (\text{with } a_0 = 1), \tag{60}$$

and the hodograph equations read

$$(u \pm \eta)_t + (u \pm 1)(u \pm \eta)_x = 0. \tag{61}$$

Thus

$$u \pm \eta = \text{const} \quad \text{along} \quad C^{\pm}. \tag{62}$$

This means that u and η are known exactly at the intersection of two characteristics, and only the position of the intersection remains to be calculated; this has been done to a second approximation. Computational precision was estimated at about 1% over a relatively long time interval, and distributions at given times were again interpolated linearly in the network of characteristics.

3. Higher-Order Front Conditions

For most of the initial conditions for which von Hagenow has previously made calculations, a second shock wave front (moving to the rear) was formed on the C^- characteristic which arises at the front point at the starting time. We believe that this can be avoided by a suitable choice of the initial distribution and that only those initial distributions are meaningful which do not form such a front. Since similar conditions can also occur in other calculations, we wish to insert a general discussion of front conditions.

Front conditions (59) are assumed to apply along the front, from which we can eliminate front velocity V,

$$u^2 = \varrho + \frac{1}{\varrho} - 2. \tag{63}$$

If we now define a function f(x,t) with

/409

$$f = u^2 + 2 - \frac{1}{\varrho} - \varrho, \tag{64}$$

then the front condition reads

$$f = 0. \tag{65}$$

Since this is to apply to all times, however, the derivative of f must also vanish along the front:

$$\frac{\partial f}{\partial t} + V \frac{\partial f}{\partial x} = 0 \quad \text{for} \quad x = X(t) = \text{position of front} \tag{66}$$

We shall call (66) a first-order front condition; thus normal front conditions (59) and (63) become zeroth order front conditions. By further differentiation in the direction of V, it is possible to derive front conditions of increasingly higher order in the same manner.

If we substitute (64) into (66), we obtain a formula which still contains partial time derivatives u_t and ρ_t. If we eliminate these time derivatives with the aid of basic equation (57), we obtain the following as a first-order front condition after several intermediate calculations:

$$\frac{\eta_x}{u_x} = \frac{V}{3} \cdot B, \qquad B = \frac{1 + 3/V^2}{1 + 1/3V^2}, \tag{67}$$

$$B \approx 1 \text{ for } V \gg 1. \tag{68}$$

We now return to the choice of initial distribution. If the boundary is supposed to represent a front at t = 0, normal front conditions (59) must of course apply there. If this were not so, the boundary point would be singular with respect to its values of u and η. If the boundary is also supposed to already have been a front shortly before (t = -ε), the first-order front condition

(67) must also be satisfied. If this were not the case, the boundary point would be singular with repect to the first derivatives.

The same argument can of course be extended to higher and higher derivatives, but these have less and less practical importance. Thus it was found for the fronts calculated in Section IIA that a second front is generated on the C^- characteristic originating from the zero point only if the normal front conditions are violated at the beginning. Now the isothermal fronts are apparently somewhat more sensitive and also demand the initial satisfaction of the first-order front conditions. But this then seems to be sufficient. Condition (67) was satisfied quite well in one of the initial distributions calculated; this was the one distribution for which a second front was not generated. We must thus be careful that we do not select any initial distributions which are singular in the sense that the front was not a front in the past.

4. Results

/410

The most striking aspect of the examples calculated was that velocity became a linear function of position after a brief time (within the limits of computational precision). The logarithm of density, η, also almost became linear, with a barely perceptible curvature. As an example, we show the same distribution at two different times in Fig. 11. The slopes of the curves (close to the front) obey equation (67) here, from which we see that the two curves cannot be made to coincide with the curves for a different time by means of the same scale transformation, as could be done in Section II,A,4.

In a manner analogous to Section II,C, von Hagenow has also studied the class of linear solutions for the isothermal case. The general solution can again be given, but it also does not

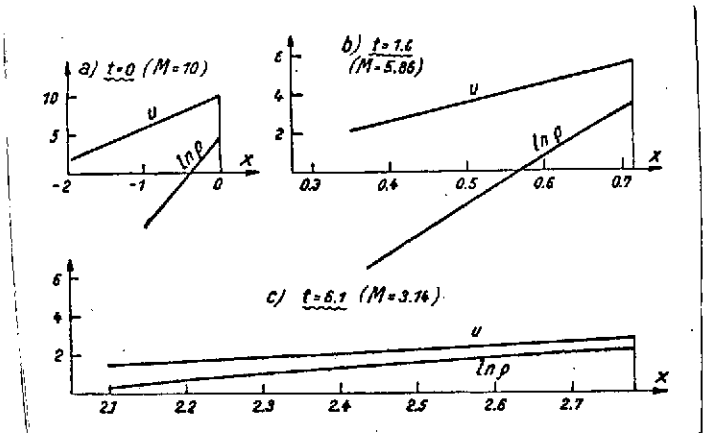

Fig. 11. Example of the development of a nonsteady isothermal front with time (u = gas velocity, ρ = density). a) initial distribution; b) and c) distributions at different time intervals. Other initial distributions yield the same distributions as these for a given Mach number M (after an adjustment period). From [28].

satisfy the front conditions. Thus, for the distribution which is established, velocity cannot be exactly linear in x, but the linear solutions do seem to be well suited to an approximate representation of the region to the rear. In the isothermal case, no arbitrary function remains free for the linear solutions as before; η is now quadratic in x.

The following was also found. If we consider two different initial distributions, the distributions associated with equal front velocities V are equal to one another after a short "adjustment time" if we suitably normalize the x-scale. If in place of $\eta(x,t)$, for example, we now write $\eta(y,V)$, making use of $V(t)$ and $y = x - X$, we then obtain the following after a certain period of time for two different initial distributions:

$$\eta_1(y,V) = \eta_2(cy,V) \text{ with } c = \text{const}, \qquad (69)$$

and similarly for $u(y,V)$. It should be noted here, though, that /411 (69) would be trivial and would follow from (67) if u and η were linear in x. And whether (69) also covers the slightly nonlinear portion of curves u and η can still not be answered clearly enough with calculations made so far.

A somewhat more far-reaching test of the same state of affairs also provides confirmation, however. Let us consider front

velocity V as the parameter for two different initial distributions and define $t_1(V)$ as the time at which the first distribution has reached the value V and $t_2(V)$ as the time at which the second distribution has reached V. By eliminating V we then obtain a function $t_2(t_1)$. For the examples calculated, it was found that

$$t_2 = a + bt_1 \text{ with } a, b = \text{const} \tag{70}$$

in all cases after a short adjustment time. Fig. 12 shows an example. Here, the fact that $a \neq 0$ means that the two distributions require different adjustment times, and $b \neq 1$ indicates a difference in time scale for development, caused by different widths of the initial distributions, i.e. by different x-scales. This reduces to (69) and it can actually be shown that (70) and (69) mean the same thing. Here, b = c, since

$$-\frac{dV}{dt} = \left(\frac{3}{2B} - \frac{1}{2}\right) \cdot \eta_x \approx \eta_x \tag{71}$$

can be derived from the front conditions and (67), whereby the time and position scales are related to one another.

In summary, it can be said, first of all, that the isothermal front can have no time-independent standard solution as in Section II, as can be seen just from (67). Secondly, a type of time-dependent standard solution appears to exist (rather, V-dependent), and we should study whether a time-independent part can be separated from it. Thirdly, the linear solutions are good approximate representations, just as before.

A satisfactory answer to the problem of the standard solution, or a good approximate description in simple form applicable to all V, would be necessary for this chapter on isothermal fronts to be considered complete. Also necessary would be an estimate of the physical conditions under which the isothermal approximation

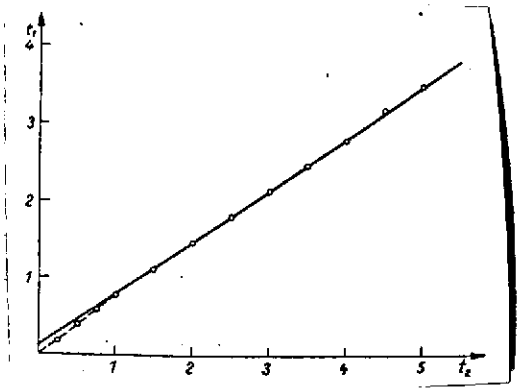

Fig. 12. Times $t_1(V)$ and $t_2(V)$ after which two different initial distributions possess front velocity V. See text regarding equation (70). From [28].

can be valid as a description of a single shock wave front. And we also should try to determine when a field of statistically distributed fronts may be described in this manner. (For example, we could ask: /412 if energy exchange by radiation is high enough for isothermal behavior, can momentum exchange by radiation still be neglected?)

IV. Steady Front in a Magnetic Field

1. Introduction

A large number of articles already exist on the presence of magnetic fields in cosmic objects and on the area of magnetohydrodynamics stemming from this and related problems; the reader is referred to the bibliographies in Lüst [34, 35]. We estimate fields on the order of 10^{-6} Gauss[4] for interstellar matter. If an ionized gas (= plasm) is in turbulent motion, electric currents arise (due to the differences in masses of electrons and ions), and thus magnetic fields are formed. In particular, all magnetic lines of force already present are eddied by the turbulence, and their density is thus increased. An exponential increase in field strength, with time, results until the energy density of the magnetic field becomes comparable to the energy density of the turbulence. From this point on, the turbulence is strongly influenced and retarded by the magnetic field (e.g. anisotropy).

[4] Higher field strengths, up to 10^{-3} or 10^{-2} Gauss, also occur in certain objects, such as the Crab Nebula.

Under conditions which occur in the cosmos, it is a characteristic of a plasma in a magnetic field that matter and lines of force practically "cling together": either the matter takes the lines of force with it as it moves (weak field) or can only move parallel to the fixed lines of force (strong field). This is caused by the fact that we can reckon with practically infinite electrical conductivity σ. We present some data in Table 4, taken primarily from an article by Schlüter [36], for comparing cosmic conductivities with metals and types of discharges on Earth.

TABLE 4. ELECTRICAL CONDUCTIVITY σ (IN esu = sec^{-1})

	log σ		log σ
Center of sun	18.3	Solar photosphere	12.9
Copper	17.7	Arc discharge	12.9
Mercury	16.0	Interstellar matter	
Solar corona	15.7	HII region	12.7
Graphite	14.6	HI region	11.8 to 10.6
Glow discharge	13.6	Window glass	-1.0
		Paraffin	-4.7

The decay time τ of a magnetic field due to ohmic losses is the criterion for evaluating conductivity:

$$\tau = \frac{l^2 \sigma}{c^2}, \qquad (72)$$

where l is a length characteristic of the magnetic field (such as the radius of curvature of the lines of force), and c is the velocity of light. Even with log σ = 10.6 for HI regions, assuming small structural details of l = 0.01 pc = $3 \cdot 10^{16}$ cm, we obtain $\tau = 10^{15}$ years. This means that we can reckon with practically infinite conductivity for times within the universe's age of $5 \cdot 10^9$ years. /413

Lüst sets up the equations in [34] for steady planar fronts of any strength in homogeneous magnetic fields of any strength and any direction, and discusses the various types of solutions in [35]. Lüst's results could again assume the role of front conditions for nonsteady fronts.

2. The Basic Equations

If friction and thermal conductivity are neglected, the basic magnetohydrodynamic equations have the following form in the steady case:

a) The equation of motion:

$$\varrho(\mathfrak{v}\ \mathrm{grad})\,\mathfrak{v} = -\ \mathrm{grad}\ p - \frac{1}{4\pi}[\mathfrak{H}\ \mathrm{rot}\ \mathfrak{H}]; \tag{73}$$

b) The equation of continuity:

$$\mathrm{div}(\varrho\,\mathfrak{v}) = 0; \tag{74}$$

c) The law of the conservation of energy can be written

$$(\mathfrak{v}\ \mathrm{grad}\ i) = \frac{1}{\varrho}(\mathfrak{v}\ \mathrm{grad}\ p), \tag{75}$$

if we designate enthalpy per unit mass as $i = e + p/\rho$.

d) For the magnetic field we also add sourcelessness

$$\mathrm{div}\,\mathfrak{H} = 0 \tag{76}$$

e) and the induction law, which under conditions in the introduction section has the form

$$\mathrm{rot}\,[\mathfrak{v}\,\mathfrak{H}] = 0. \tag{77}$$

Lüst derives the appropriate laws of conservation from these basic equations. We find that we obtain the same form as in normal hydrodynamics if, in place of pressure p, we introduce

a pressure tensor

$$p_{ik}^{*} = \left(p + \frac{1}{8\pi}\mathfrak{H}^2\right)\cdot\delta_{ik} - \frac{1}{4\pi}H_iH_k, \tag{78}$$

add a magnetic term to internal energy e per unit mass

$$e^{*} = e + \frac{1}{8\pi\varrho}\mathfrak{H}^2, \tag{79}$$

and also write enthalpy i as a tensor

$$i_{ik}^{*} = \left(i + \frac{1}{4\pi\varrho}\mathfrak{H}^2\right)\cdot\delta_{ik} - \frac{1}{4\pi\varrho}H_iH_k. \tag{80}$$

3. Front Conditions

/414

From the laws of conservation, Lüst calculates front conditions for the quantities ρ, i, v_x, v_y, H_x, H_y (x is the direction of propagation of the front; y is the direction of the projection of the lines of force on the plane of the front). Due to the complexity of the equations, we must refer the reader to the original article. In the case of oblique lines of force, they exhibit a break as they pass through the front, and we thus now have (in contrast to the front without a field) an additional tangential acceleration of the gas as the front passes through it.

An additional, more important complication is that the front conditions are no longer single-valued. For example, the equation for the jump in density is third-order. It can have three real solutions, at least one of which we ignore, though, due to the required entropy increase in the front. The remaining ambiguity then means that for a specified region ahead of the front and a specified front velocity, conditions behind the front are not

established uniquely; rather, two different types of shock wave fronts are possible under some circumstances. Because of this fact, Lüst first performs an analysis for the limiting case of vanishing shock strength (M = 1), i.e. for sonic waves.

4. Sonic Velocity in the Plasma

Due to the transverse rigidity of the magnetic field, there are three different types of sonic waves in the plasma with (generally) different sonic velocities. We show a polar diagram in Fig. 13. If we set up a perturbation at the origin at time t = 0, the three sonic waves produced lie on the plotted curves at time t = 1. The waves whose velocities are designated c_+ and c_- oscillate in the x,y-plane (defined as above) obliquely relative to the direction of propagation, i.e. are mixed longitudinal and transverse waves. The wave designated c_A undergoes pure transverse oscillation in the z-direction and is called an Alfvén wave.

Let β be the ratio of hydrodynamic internal energy e to total /415 energy e*, as given in (79), ϕ be the angle between the lines of force and the direction of propagation, and let η = cosϕ,

$$\left.\begin{aligned}\beta &= \frac{e}{e^*}\\ &= \left(1+\frac{\gamma-1}{8\pi}\frac{H^2}{p}\right)^{-1}\\ \eta &= \cos\varphi;\end{aligned}\right| \qquad (81)$$

Fig. 14 then shows the three sonic velocities as functions of β and η. We see, for example, that only for relatively weak magnetic fields do c_A and c_- differ by as little as they are shown to differ in Fig. 13.

We show all of the possible limiting cases in Table 5. The last line, for example, tells us the following: the c_- wave is generally mixed (direction of oscillation oblique to direction of

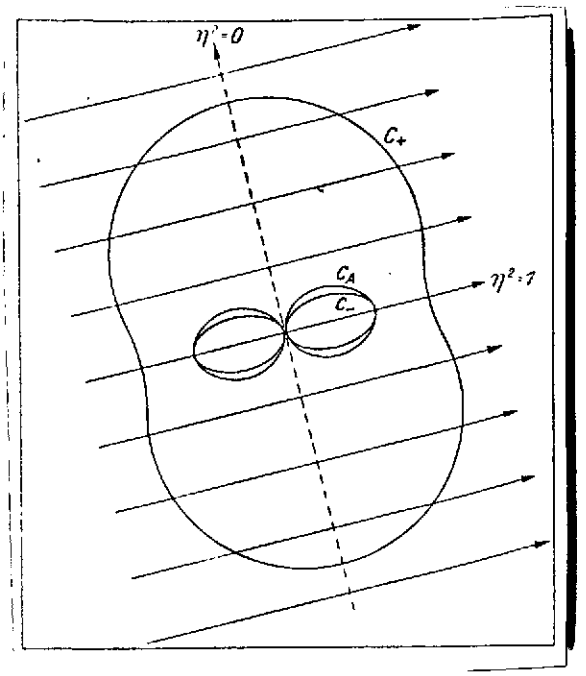

Fig. 13. Polar diagram of sonic velocities c_-, c_A and c_+ for a plasma in a magnetic field ($\beta = 0.75$, i.e. magnetic energy is 1/4 of total energy). From [35].

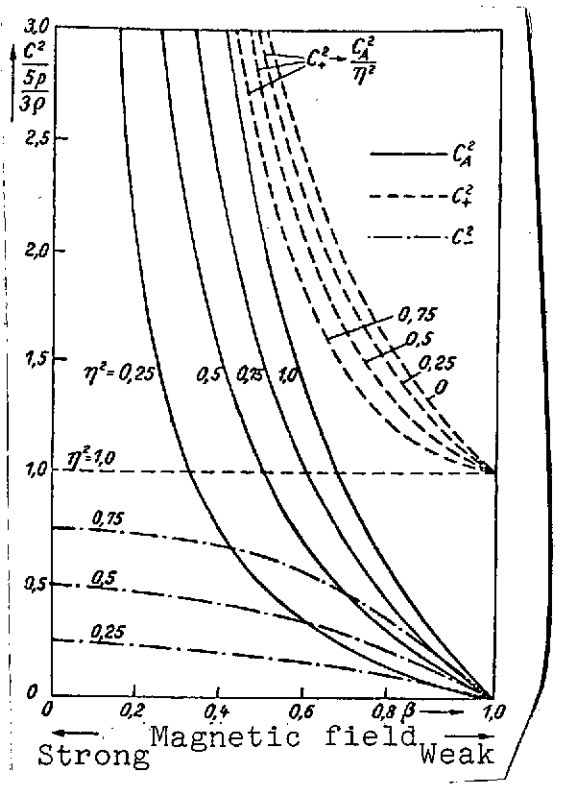

Fig. 14. The three sonic velocities as functions of the strength and direction of the magnetic field; see (81). From [35].

TABLE 5. LIMITING CASES FOR THE THREE TYPES OF SONIC WAVES

Wave type	In general	Field rel. to direction of propagation			
		∥	⊥	∥	⊥
c_+	m	$c_S(l)$	$c_g(l)$	$c_A(t)$	$c_g(l)$
c_A	t	$c_A(t)$	0	$c_A(t)$	0
c_-	m	$c_A(t)$	0	$c_S(l)$	0
		Weak field		Stong field	

$c_S^2 = 5p/3\rho$, ordinary sonic wave without field,

$c_A^2 = H_x^2/4\pi\rho$, Alfvén wave,

$c_g^2 = H_y^2/4\pi\rho$, limiting case for c_+ wave,

l = longitudinal,

t = transverse,

m = mixed.

propagation); in a parallel weak field, its velocity is equal to that of the Alfvén wave, and the direction of oscillation is purely transverse. In a parallel strong field, its velocity is equal to sonic velocity without the field, and the direction of oscillation is purely longitudinal. The velocity of the c_- wave becomes zero in a perpendicular field in each case, and

$$c_A \ll c_S \text{ in a weak field,} \qquad (82)$$
$$c_A \gg c_S \text{ for a strong field.}$$

5. Discussion

The presence of the three different types of sonic waves in a plasma can be considered certain. It is not clear, on the other hand, whether the corresponding three different types of shock fronts can actually be realized physically. In Fig. 15 we show the density jump in the front as a function of front velocity V for a relatively strong magnetic field. Accordingly, a front (corresponding to the c_- sonic wave), which we have labeled F_-, exists at $V \geq c_-$; the jump in density initially increases. The other two solutions begin below $\rho_2/\rho_1 = 1$; they would thus be connected with an entropy decrease and are thus physically impossible. Only beyond $V = c_A$ can we add front F_A (corresponding to the Alfvén wave). As V increases, the density jump in F_A increases and that in F_- decreases, until both finally coincide at $V = V_g$. No shock wave front exists at all from there to $V = c_+$; front F_+ only occurs beyond $V = c_+$. From there on the density jump increases monotonically and approaches the limiting value $\rho_2/\rho_1 = 4$ asymptotically (just as for a strong front without a field).

It appears somewhat incredible that an interval $V_g < V < c_+$ should exist in which no shock wave fronts are possible, while shock wave fronts still exist at lower velocities (in the

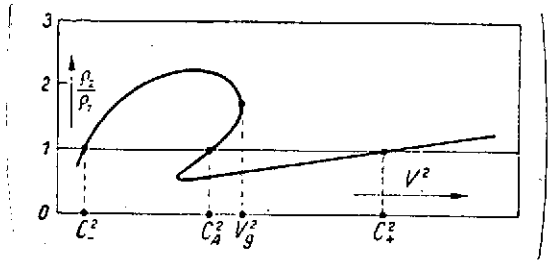

Fig. 15. Density jump in the front as a function of front velocity V for $\beta = 0.25$ and $\eta^2 = 0.5$; see (81). From [35].

interval $c_- < V < V_g$). What happens, for example, to an F_- front continually accelerated from behind as it passes V_g? It is generally characteristic of a shock wave front that it is faster than the perturbation waves emanating from it, i.e. it moves into an undisturbed region to the front of it. A study should therefore be made as to whether the F_- and F_A fronts are perhaps physically impossible because c_+ waves might be excited by them which move more rapidly than the front itself. That would then mean that shock wave fronts can only form via the highest of the three sonic velocities, c_+. Clarification of these questions would be very desirable.

V. The Interaction of Nonsteady Fronts

1. Introduction

The problem of the interaction of shock wave fronts plays a critical role in the working program which we set up at the beginning (turbulence with supersonic velocities). The actual objective here would be to obtain the simplest possible general information regarding the interaction of shock wave fronts of any strength and direction, also taking energy radiation (and possibly magnetic fields) into consideration. The article by K. Hain [37] can be considered a first step in this direction; he calculated a number of examples numerically which involve two planar, parallel, nonsteady fronts which collide or overtake one another, without energy radiation loss and without magnetic fields. The overtaken front or, in the case of collision, both fronts are assumed to be strong and of the type associated with the standard solution; the undisturbed region ahead is quiescent and of constant density and negligible temperature.

Since the complexity and extent of computations almost exceeded the capacity of the one G 1 computer available at that time, only a relatively small number of examples -- six -- could be computed. It was therefore also not yet possible to get much farther than theorems and suppositions with respect to the requirement for a general and simple description. The results are represented in the original article in the form of numerous figures which indicate the spatial and temporal behavior of the variables of state. We can only present a brief summary here.

As in [6], calculations were again made using the method of characteristics, with differential satisfaction of the front conditions for any front strength; the front conditions were

solved by iteration. The state variables at the space-time point of collision (or overtaking) are obtained from the equations of Courant-Friedrichs [14] applicable to steady shock waves.

2. Collision

In Fig. 16a we show the space-time point of collision and its vicinity. V^+ and V^- are the velocities of the two incoming fronts. Two outgoing fronts are formed, plus a discontinuity surface at which density and temperature change discontinuously while pressure and velocity remain continuous.

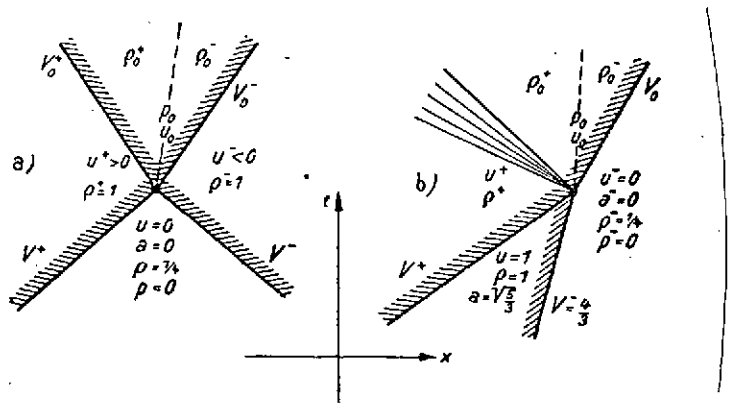

Fig. 16. Interaction between two shock wave fronts. a) Collision, b) one overtaking the other.
——— Shock wave front, denser side hatched;
----- Discontinuity surface.
Centered rarefaction wave shown as a pencil of lines. From [37].

In order to characterize the strength ratio of the incoming fronts, we define

$$F = -V^+/V^- = -u^+/u^- \quad (83)$$

The discontinuity surface vanishes for fronts of equal strength ($F = 1$). The two outgoing fronts can no longer be approximated as strong fronts, since the density jump is now only by a factor of 2.5, as compared to a factor of 4 for a strong front. Thus density increases by a total factor of $\rho_0^-/\rho = 10$ relative to the undisturbed region ahead. Pressure increases by a factor of 6 and temperature by a factor of 2.4 at the outgoing front. /418

If the shock wave fronts are very unequal, on the other hand, e.g. F >> 1 (but both Mach numbers large relative to 1), the stronger of the two fronts continues almost unchanged as a strong front, whereas the weaker of the two proceeds with a density jump of $\rho_o^+/\rho^+ = 1.5$ after collision. Maximum density increase is now $\rho_o^-/\rho = 16$ for F >> 1. The timewise development of front values can be described as follows. Density decreases rapidly in all cases, since each front is passing into the region of decreasing density behind the other. The situation is different in the case of front velocity: were the front to pass into a quiescent, constant region, front velocity would drop off. This is opposed by the facts, first, that the density of the region ahead of the front decreases and, secondly, that gas velocity in the region increases in the direction of front velocity. The behavior shown in Fig. 17 results: only in the case of a very unequal strength distribution does the velocity of the stronger front (F = 4) decrease with time, whereas for F ≤ 1, the effect of the region ahead predominates, and a pronounced increase in front velocity with time results. Temperature at the front decreases monotonically for F = 2 and F = 4, while for F ≤ 1 it initially rises somewhat and only then falls off.

/419

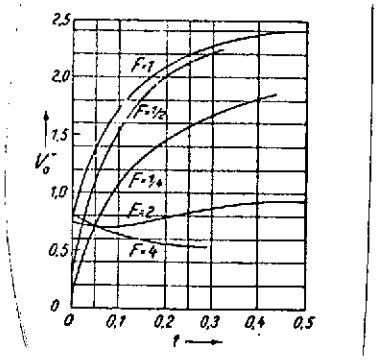

Fig. 17. Front velocity V_o^- as a function of time after collision. F from (83). Normalization: $u^+ = 1$ for F ≥ 1, and $u^- = 1$ for F ≤ 1. From [37].

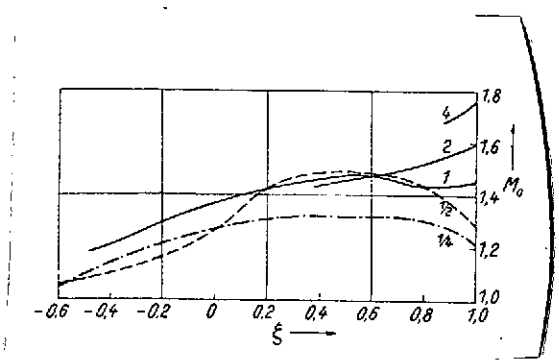

Fig. 18. Front strength M_o, as defined by (84), after collision as a function of homology variable ξ for the region ahead of the front. Timewise development proceeds from right to left. From [37].

Hain proposes that the timewise development of the front values not be plotted over time itself but over the homology variable ξ defined by (25) for the region ahead. (The homologous standard solution was assumed for this region ahead, i.e., the region behind the opposing front.) When this type of plot is made, it appears as if fronts of all strengths would, after initial differences, ultimately approach the same timewise behavior.

As an example, we show the timewise behavior of the quantity

$$M_0 = \frac{V_{\bar{0}} - u^-}{a_{\bar{0}}} \Bigg| \tag{84}$$

in Fig. 18 as a function of ξ; M_0 represents a measure of the strength of the outgoing front. $M_0 \to 1$ in the limiting case of the weak front; $M_0 \to 4/\sqrt{5} = 1.79$ in the limiting case of the strong front. (The quantity M_0 was erroneously designated as Mach number in [37].) It appears as if all fronts would stop at about the same ξ value ($M_0 = 1$), at approximately $\xi = -0.7$. A further study of this problem would be of interest, particularly for the collision statistics which are to be applied.

The spatial distribution of the variables of state in the region behind the front is shown by Hain in a large number of figures. While velocity deviates only slightly from linearity, the other quantities differ greatly from the standard distribution, since no free flowoff can occur to the rear, and since the region ahead is not constant. Temperature decreases continuously to the rear, density generally increases.

3. One Overtaking Another

Figure 16b shows the space-time point of overtaking and its vicinity. A forward-moving shock wave front, a discontinuity

surface and a rearward-moving centered rarefaction wave are generated according to [14]. If the density jump is $\rho^+/\rho > 1.6$, the resultant front is faster than the original front.

The standard solution was always employed in numerical computation for the overtaken front (V^-) and the region behind it. The overtaking front (V^+) was likewise used in the form of the standard solution at the beginning of calculation, but subsequent calculation was done with the method of characteristics in the nonsteady mode. The overtaking front decays so rapidly with time that it could not be followed beyond the time of overtaking in two computed examples.

It is worth noting that here, too, linear velocity distributions are again set up in all cases, both behind the overtaking front (V^+) and behind the generated front (V_o). The tendency /420 toward linear flowoff thus appears to be very general and dominant.

The results of the calculations can be represented as follows: If the overtaking front is weak, the overtaken front is modified to only a very slight degree. If the overtaking front is strong, the standard solution is likewise established again behind the generated front after a certain period.

4. Summary

1. When one front overtakes the other, the standard solution is always established a certain length of time after interaction.

2. After collision, the subsequent behavior of the fronts appears essentially to be determined only by the homology solutions into which they pass. All fronts appear to have decayed to $M_o = 1$ at about $\xi = -0.7$, but this still remains to be confirmed by additional calculations.

3. All velocity distributions generated are approximately linear.

Addendum: A restriction is necessary regarding item 2. If we define the width w of a front at the instant of collision t_o by

$$w = |X - x_{1/2}| \text{ and } \varrho(x_{1/2}, t_0) = (1/2)\,\varrho(X, t_0),$$

then the width ratio has always been taken as $W = w^+/w^- = 1$ in the examples calculated by Hain. For a complete description, however, not only front strength ratio F but also width ratio W would actually have had to vary. In going to a limiting case, e.g. $W \to 0$, we see that statement 2 (all fronts have decayed to $M_o = 1$ at the same ξ) can then no longer hold.

VI. Statistical Model of a Field of Shock Wave Fronts

1. Introduction

The goal of our working program was first to study the individual problems of shock wave fronts and their interaction and to answer them with the most general and simplest possible statements. These results were then to help in describing, completely and statistically, a field of shock wave fronts passing through one another. In particular, processes involved in the establishment of equilibria or steady states were to be studied, and we can seek an ultimate state of equilibrium established with a suitable input of energy. This statistical description of an equilibrium approached asymptotically should then serve as a basis for a theory of supersonic turbulence.

In the preceding sections we reported on the studies concerning the individual problems. If we consider the selection of problems studied and the scope of the results obtained, it might seem premature to begin now with a statistical description. In particular, we are still missing a study of the interaction of fronts intersecting obliquely and of the effect of energy radiation (and possibly of magnetic fields) upon interaction. /421 Sufficient material is not yet available in Chapters III (radiation loss) and V (interaction), and that which is available has not yet been worked through sufficiently to allow adequate representation in simple and general statements. Moreover, only infinitely extended fronts have been studied so far, whereas we require the timewise development and the interaction of spatially restricted fronts for the statistics of a shock wave front field.

If we nevertheless make an attempt now at a statistical description of shock wave front fields, we do so for two reasons. First, the general behavior of a shock wave front field can already be studied qualitatively with a very crude model. We can use it to see, say, how an equilibrium state might look, and

when and how it would be established. In addition, we obtain a feeling for the initial data on which it essentially depends. The second reason is of a technical nature: even the execution of a very crude model practically exceeded the capacity of the Göttingen G 2 computer, and the execution of a considerably improved model would be quite hopeless at this time. In the following we describe work by Irene Crone [38] on a very simplified statistical model.

2. The Model

In order to limit computational outlay, which increases sharply with the number of dimensions, the velocity and size of the fronts were considered in only one dimension, the position of one front in two dimensions. All fronts lie parallel to the y,z-plane and move in the x direction. They are of infinite size in the y- and z-directions. We do not consider the processes occurring in a volume, but only the lines of intersection of the fronts with the x,y-plane, so the size of the fronts in the z-direction does not play a role. We consider only a fixed rectangle; fronts which leave this region at one boundary are reintroduced at the opposite boundary at a random location with the same variables of state.

Each front is characterized by two quantities: velocity (in the x-direction) and length (in the y-direction). Velocity decreases with time, as $t^{-0.4}$, as an approximation to the standard front. This means that we assume a spatially and temporally constant average for all variables of state for the region ahead of each front. New fronts, discontinuity surfaces and expansion waves are generated by interaction (in accordance with the formulae from [14]); all possible interactions among these three types of objects are taken into consideration. In the examples calculated, the total number N of all objects lay within the

interval 50 < N < 1000. As an example, we show the collision of two fronts with partial overlap in Fig. 19.

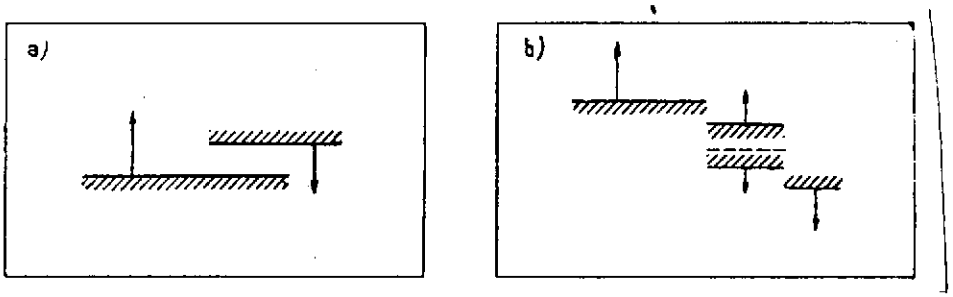

Fig. 19. Model collision between two fronts. A) Before, b) after. Four smaller fronts and a discontinuity surface are produced. From [38].

Small fronts are always produced from large fronts. This process has a lower limit in nature, since very small fronts disintegrate rapidly ("break up" from the edge inward); this is taken into consideration in the model, as a rough approximation, by the introduction of a "minimum length." All fronts /422 which are produced below this length are simply deleted. Likewise, all fronts are deleted which have dropped to Mach numbers less than 1.5 in the course of time.

The energy input necessary for a steady state is provided by the fact that a certain number of large and fast fronts are reintroduced per unit time at the boundaries of the region, with Mach numbers up to M = 25.

The model includes a number of parameters which can be selected freely, e.g. the frequency of energy input, the frequency distributions of the lengths and velocities introduced, the ratio of the largest to smallest length, etc. The most important of the free parameters, however, is provided by the ratio of mean collision time to the time scale of the

velocity drop of the fronts. This parameter is defined by

$$\alpha = \frac{V(t_0 + \tau_0)}{V(t_0)} = \left(1 + \frac{\tau_0}{t_0}\right)^{-0,4} \quad (85)$$

in I. Crone's work. Here V(t) is front velocity, decreasing with time as $t^{-0.4}$; t_0 is the "age" at which all fronts in the energy input are reintroduced; and τ_0 is mean collision time (at the beginning of a computational example). The significance of α will be illustrated with the extreme cases. If $\alpha \to 0$, then practically no collisions occur; the fronts fed in simply die out by "aging." If $\alpha \to 1$, then practically no "aging" occurs; the introduced fronts chop one another down to minimum length in a short time. After several preliminary trials, $\alpha = 0.6$ was selected; reasonable processes of steady state development were obtained in the vicinity of this value.

3. Execution

The problem was solved by Monte Carlo methods, since the differential equations both for the process of establishing a steady state and for the steady state are hopelessly complex. The necessary random data were continually generated during computation by a method proposed by the author in [39].

Some pairs of fronts available in a "list" are selected by random decision. A probability P is calculated for the interaction of two such fronts from the two velocities and lengths. /423
A random number (equally distributed within a certain interval) is now generated. If probability P lies above this random number, interaction occurs; if it lies below, two other fronts are selected. When interaction occurs, the two old fronts are deleted from the list; the products of interaction are calculated and entered in the list. In addition, a new front is added at statistically distributed time intervals (energy input), the variables of state

for which are random values from predetermined distributions of length and velocity. All of these processes were taken care of by a fully automatic program on the G 2.

4. Results

In the following figures we present a number of the results from four examples which were executed. If we designate the number of shock wave fronts added per unit time as Z, then

$$Z_D : Z_C : Z_F : Z_E = 1:2.1:2.1:4.2,$$

and the values of α are

$$\alpha_C = \alpha_D = \alpha_E = 0.60 \text{ and } \alpha_F = 0.75.$$

Velocities are equally distributed over an interval $0.75\ V_{max} \leq V \leq V_{max}$ at the beginning of computation and in the introduction of new fronts, and likewise for the lengths. The Mach number is M = 25 at V_{max} here, and $r_{max}/r_{min} = 10$. /424

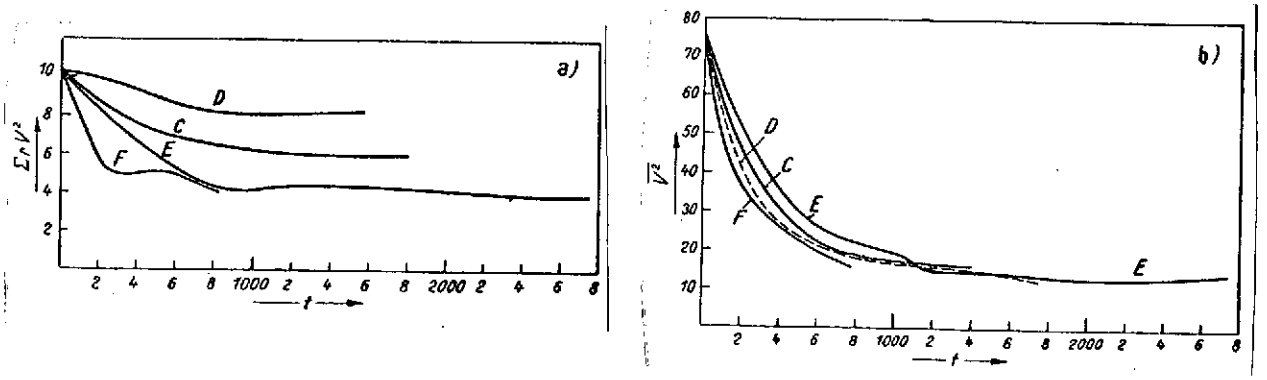

Fig. 20. Process of steady state establishment in a field of shock wave fronts. a) Total energy ΣrV^2 over time t. b) Mean square velocity over time t. From [38].

In all four examples, all mean values and likewise all distributions approach an equilibrium state after a certain length of time. In Fig. 20a we see the timewise development of "total energy" ΣrV^2 contained in the region under consideration

(r = length, V = velocity, summed over all fronts, discontinuity surfaces and rarefaction waves). Figure 20b shows the development of mean square velocity V^2. A striking feature is that the mean velocity which is established hardly depends upon the parameters, and is about equal to half the velocity of the fronts added. On the other hand, total energy (for a given α) decreases approximately with $\sqrt{Z}$, since pronounced dissipation results from the "chopping up" effect accompanying a high input level.

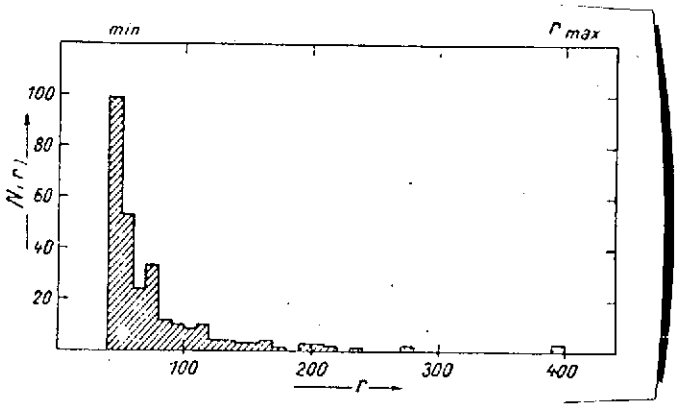

Fig. 21. The distribution N(r) of front lengths r which is established in example C. The result is about the same in the other examples, too. From [38].

Figure 21 shows the distribution of length r which is established in example C. Practically the same distribution is also eventually established in the other examples. The distribution increases sharply toward the smallest fronts; we see from this that cutting off at a "minimum length" represents a somewhat forced simplification of our model.

It was found that this model is thoroughly suitable for studying processes in the assumption of a steady state in a field of shock wave fronts and that it is reasonable to seek an equilibrium state and to try to describe its characteristics statistically. Moreover, the usability and superiority of the Monte Carlo method used is confirmed for the problem at hand.

In closing, we would again like to express the hope that the problem treated here will be attacked again in another study group. To this end, the interaction of oblique fronts with

energy radiation should probably first be studied, perhaps making use of the limiting case of the isothermal front. An additional /425 point yet to be clarified is the timewise development of fronts of finite extent. A three-dimensional model improved in this respect should then be capable of providing quantitative information for the theory of supersonic turbulence being sought. To be sure, it could only be executed on an extremely fast and large computer.

I would like to cordially thank Prof. von Weizsäcker and all members of our study group for many discussions and for a number of unpublished works which were obligingly made available to me.

REFERENCES

1. Heisenberg, W., Z. Phys. 124, 628 (1947).
2. v. Weizsäcker, C.F., Z. Phys. 124, 614 (1947).
3. Chandrasekhar, S., Proc. Roy. Soc. A 229, 1 (1955).
4. Chandrasekhar, S., Phys. Rev. 102, 941 (1956).
5. v. Weizsäcker, C.F., Z. Naturforsch., 9a, 269 (1954).
6. Hain, K. and S. v. Hoerner, Z. Naturforsch. 9a, 99 (1954).
7. Taylor, G.I., Proc. Roy. Soc. A 201, 159 (1950).
8. Guderley, G., Luftfahrtforsch. 19, 302 (1942).
9. Guderley, G. Z. Angew. Math. Mech. 22, 121 (1942).
10. v. Hagenow, K.U., Dissertation, Göttingen, 1956, unpublished.
11. Lie, S. and F. Engel, Ges. Abhandlungen, Vol. IV, see p. 358.
12. Lax, P., Commun. Pure Appl. Math. 7, 159 (1954).
13. Häfele, W., Z. Naturforsch. 10a, 1006 (1955).
14. Courant-Friedrichs, Supersonic flow and shock waves, New York, 1948.
15. Tollmien, W.,Z. Angew. Math. Mech. 11, 117 (1937).
16. Tollmien, W., Z. Angew. Math. Mech. 21, 140 (1941).
17. Häfele, W., Z. Naturforsch. 10a, 1017 (1955).
18. Taylor, I.L., Phil. Mag. 46, 317 (1955).
19. Culler, G.J. and B.D. Fried, ARL-6-20 (Ramo Wollridge Corp., Los Angeles).
20. Häfele, W., Z. Naturforsch. 11a, 163 (1956).
21. v. Hoerner, S., Z. Naturforsch. 10a, 687 (1955).
22. Burgers, J.M., K. Ned. A. Wetensch. 49, 588 (1946).
23. Pack, D.C., Monthly Notic. Roy. Astron. Soc. 113, 43 (1953).

24. Meyer, F., Z. Naturforsch. 10a, 693 (1955).

25. Häfele, W., Z. Naturforsch. 11a, 183 (1956).

26. Pikelner, S.B., Ber. Sternwarte Krim 12, 93 (1954).

27. Hertweck, F., Master's thesis, Göttingen, 1956 (unpublished).

28. v. Hagenow, K.U. (unpublished, 1956).

29. Chamberlain, J.W., Astrophys. J. 117, 387 (1953).

30. Petschek, H.E., P.H. Rose, H.S. Glick, A.Kane and A. Kantrowitz, J. Appl. Phys. 26, 83 (1955).

31. Lin, S.C., E.L. Resher and A. Kantrowitz, J. Appl. Phys. 26, 95 (1955).

32. Bond, J.W., Jr., Phys. Rev. 105, 1683 (1957).

33. Weber, O., Z. Phys. (in press).

34. Lüst, R., Z. Naturforsch. 8a, 277 (1953).

35. Lüst, R., Z. Naturforsch. 10a, 125 (1955).

36. Schlüter, A., Z. Naturforsch. 5a, 72 (1950).

37. Hain, K., Z. Naturforsch. 11a, 329 (1956).

38. Crone, I., Dissertation, Göttingen, 1957 (unpublished).

39. v. Hoerner, S., ZAMP 8, 26 (1957).